THE ROLE OF HMGN1 IN NUCLEOTIDE EXCISION REPAIR OF HUMAN CELLS: MECHANISMS AND POSSIBLE APPLICATIONS

A DISSERTATION

SUBMITTED IN PARTIAL FULFILLMENT OF THE REQUIREMENTS

FOR THE DEGREE OF DOCTOR OF PHILOSPHY

IN THE GRADUATE SCHOOL OF THE

TEXAS WOMAN'S UNIVERSITY

BIOLOGY DEPARTMENT

COLLEGE OF ARTS AND SCIENCES

BY

LATONDRA J. LAWRENCE, B.S.

DENTON, TEXAS

DECEMBER 2015

TEXAS WOMAN'S UNIVERSITY
DENTON, TEXAS

November 9, 2015

To the Dean of the Graduate School:

I am submitting herewith a dissertation written by LaTondra J. Lawrence entitled "The Role of HMGN1 in Nucleotide Excision Repair of Human Cells: Mechanisms and Possible Applications." I have examined this dissertation for form and content and recommend that it be accepted in partial fulfillment of the requirements for the degree of Doctor of Philosophy with a major in Molecular Biology.

Michael Bergel, Ph.D., Major Professor

We have read this dissertation and recommend its acceptance:

Interim Department Chair

Accepted:

Dean of the Graduate School

ACKNOWLEDGEMENTS

The fulfillment of this dissertation has been the most rigorous yet exciting challenge I have ever had to face. I would never have been able to complete this journey without the patience and guidance of several people. It is to them that I owe my deepest gratitude.

I would like to first express my sincere gratitude to my mentor Dr. Michael Bergel for giving me a chance and welcoming me into his lab. I would also like to thank him for his continuous support, time, encouragement, and guidance during the course of my Ph.D. study. His guidance helped to make me a better student, researcher, and writer. He provided me with the tools necessary to be the best and without him it would have been impossible to reach this goal.

I would also like to thank my committee members, Dr. Mary Anderson, Dr. Heather Conrard-Webb, Dr. Camelia Maier, and Dr. Nathaniel Mills for their time, insightful comments, encouragement, and valuable input.

I would also like to express my gratitude to Dr. Sarah McIntire, former chair of the Department of Biology, for accepting me and allowing me an opportunity to obtain my Ph.D. degree at Texas Woman's University.

I would also like to thank Ms. Reta (Smiddy) Foreman for providing me with an opportunity to become a better teacher and leader and for her continuous support and encouragement during this process.

I would be remiss if I did not thank all my fellow labmates for their support, collaboration, and friendships during this process. Thank you to former and current graduate students: Dr. Mangalam Subramanian, Dr. Hemangi Patil, Dr. Sudheer Dhanireddy, Rhiannon Gonzalez, Carrie Wilks, Amon Gekombe, Loni Puckett, and Mohammad Abbas. I would also like to thank the undergraduate student and high school student who helped with my research along the way: Wubet Gebre-Hiwot and Kathryn Hokamp.

A huge thank you is also necessary to Dr. Lynda Uphouse and the MBRS program. Dr. Uphouse was a huge support and encouraged and challenged me to be my best. The MBRS program allowed me the awesome opportunity to focus solely on my research and classwork for several years during my Ph.D. studies, and also afforded me the opportunity to attend multiple conferences to network with others in my field, a truly unforgettable opportunity.

A special thank you also is required for my graduate student mentor, the late Dr. Angela Peterson-Ford. She motivated and encouraged me daily and was an inspiration.

I would also like to give many thanks to my mother Sherry Lawrence who helped and encouraged me to pursue my dreams of higher education. Her support was unwavering and I am happy to be able to share this moment with her.

Finally, I would like to dedicate this degree to my father Harold Lawrence. I know that I have his support always and hope that he is smiling and watching as I complete this momentous occasion.

ABSTRACT

LATONDRA J. LAWRENCE

THE ROLE OF HMGN1 IN NUCLEOTIDE EXCISION REPAIR OF HUMAN CELLS: MECHANISMS AND POSSIBLE APPLICATIONS

DECEMBER 2015

High Mobility Group Nucleosomal binding proteins (HMGNs) are a group of non-histone chromosomal proteins that serve as architectural proteins. They modify the chromatin by transiently binding to the nucleosomal core particles, thus allowing regulation of transcription, replication, and DNA repair. Following UV irradiation of cells, the nucleotide excision repair (NER) pathway is activated to remove the bulky adducts formed. This process requires unfolding of the chromatin at the damage sites to allow accessibility of the repair complexes, and refolding of chromatin following the repair. HMGN1 may play a role in NER by recruitment of repair modulators such as HATs and HDACs to the damage site or to the chromatin globally. This study investigated the role of HMGN1 in nucleotide excision repair by employing HeLa cells that overexpress HMGN1. Here we show that overexpression of HMGN1 but not HMGN2 leads to a significantly higher cell survival rate following UV irradiation as compared to control HeLa cells. Overexpressing HMGN1 did not confer a growth advantage to HeLa cells and

Southwestern analysis experiments demonstrated a significant increase in the repair capacity of the HMGN1 overexpressing HeLa cells, suggesting the importance of HMGN1 in nucleotide excision repair in human cells. The HMGN1 overexpressing cells showed an increased post-UV global core histone deacetylation rate at histones at H4K5, H3K14 and H3K9. We observed global deacteylation that peaked 4-10 hours after UV irradiation in cells overexpressing HMGN1 and in control HeLa cells. We also showed by co-immunoprecipitation and pull-down assays, that HMGN1 is associated with the histone acetyltransferases p300 and histone deacetylase HDAC2. Our results support the hypothesis that HMGN1 recruits HATs and HDACs to the chromatin in a specific sequence after UV irradiation. Confocal microscopic analysis by local UV irradiation demonstrated partial colocalization of HMGN1 with XPC, 5 minutes and 1 hour following UV irradiation and colocalization of HMGN1 with PCNA, 24 hours following UV irradiation. Together these results suggest that HMGN1 functions in both the beginning and end of the nucleotide excision repair pathway by targeting histone acetyltransferases and histone deacetylases to chromatin globally and locally in a sequential manner following UV irradiation.

TABLE OF CONTENTS

Page

LIST OF TABLES

Table Page

LIST OF FIGURES

Figure Page

CHAPTER I

INTRODUCTION

Cellular Response to DNA Damage

DNA damage is a common event that can lead to mutations or deletions within chromosomal DNA. These mutations or deletions can occur during replication, transcription, or following damage to the DNA caused by various genotoxic agents (Narlikar, G.J et al., 2006; Watson J.D. et al., 2014) and they can lead to cancer or premature aging. This damage induces several cellular responses including checkpoint arrest, DNA repair, and triggering of apoptotic pathways (Kao et al., 2005). Damage to the DNA can be caused by endogenous and exogenous agents. Endogenous agents can cause: oxidation of bases, alkylation of bases, deamination, depurination, hydrolysis of bases, and mismatch of bases. Exogenous agents that lead to DNA damage include: UV light, ionizing radiation, thermal disruption, and certain industrial and environmental chemicals (Friedbergy E.C. et al., 2006; Narlikar, G.J et al., 2006; Watson J.D. et al., 2014). Once DNA damage is caused, there are several repair pathways that may be activated, these include: direct reversal, DNA mismatch repair, base excision repair, nucleotide excision repair, double stranded DNA repair, and more (Friedbergy E.C. et al., 2006; Wyrick and Roberts, 2015).

However for repair to occur the repair pathways must be able to recognize and respond to a wide range of damage.

Nucleotide Excision Repair (NER) Pathway

This research focuses on the nucleotide excision repair (NER) pathway. This pathway acts on a variety of DNA lesions and differs from other repair pathways in that it repairs DNA damage affecting single strands and longer sequences of bases (usually 2-20 bases). The common features among the DNA lesions recognized by the NER pathway is that they tend to cause both a helical distortion of the DNA duplex and a modification of the DNA chemistry/structure (Kao et al., 2005). Cyclobutane pyrimidine dimers (CPDs) and pyrimidine (6-4) pyrimidone photoproducts (6-4PPs) are the two main types of photoproducts caused by UV irradiation and repaired via the NER pathway (van Steeg and Kraemer, 1999; Volker et al., 2001). Both photoproducts are caused when the bases of linked nucleotides are improperly cross-linked, giving rise to bulky DNA adducts. CPDs induce a DNA bend or kink of 7-9° and 6-4PPs induce a bend or kink of 44° (Ura and Hayes, 2002) (Figure 1).

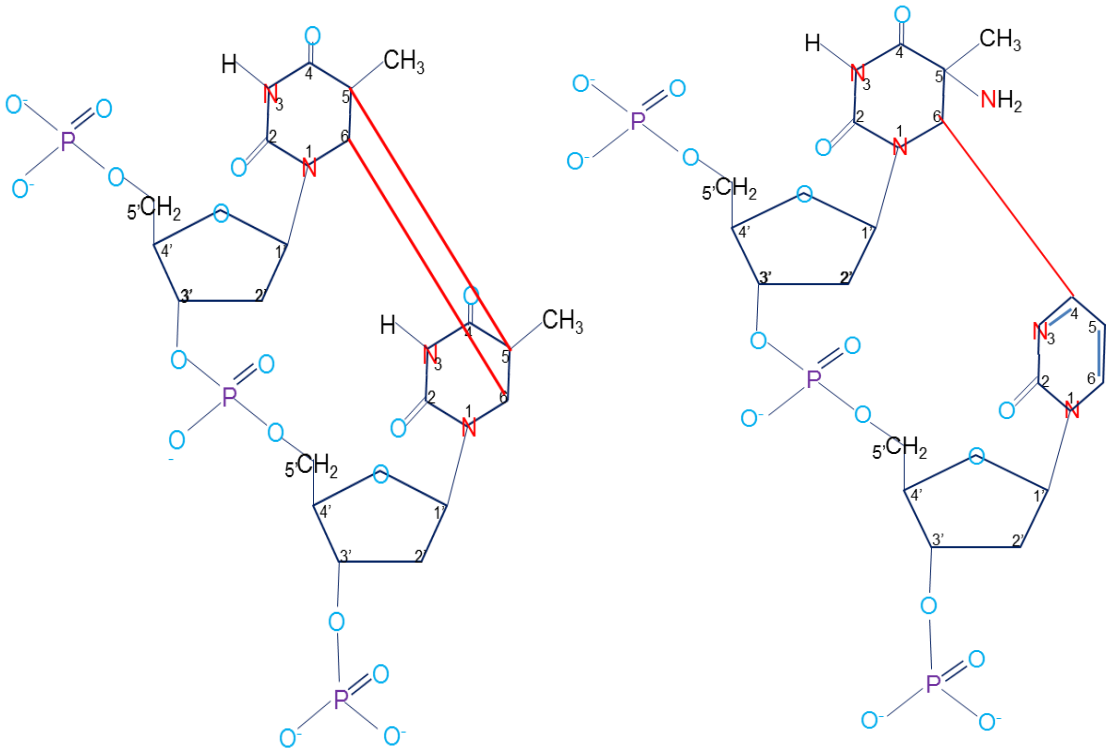

(A) Cyclobutane pyrimidine (B) 6-4Photoproducts

Figure 1: Two Main Types of Photoproducts Caused by UV Irradiation
Red lines depict the cross-linked bases on adjacent nucleotides on the same DNA strand.
Adapted from: van Steeg and Kraemer, 1999

The nucleotide excision repair pathway is a multistep process that involves more than 30 different proteins, some of which are also known to participate in transcription and replication (Aboussekhra and Thoma, 1999; Petruseva et al., 2014). The basic sequence of this pathway is as follows: (i) recognition of DNA damage, (ii) unwinding of the DNA around the lesion, (iii) dual incision of the DNA on both sides of the damage, (iv) removal of the excised oligonucleotide, and (v) filling of the generated gap by DNA polymerase and ligase (Zotter et al., 2006). The NER pathway is divided into two separate subpathways, transcription-coupled repair (TCR) and global genome repair (GGR) (Figure 2). TCR is the subpathway by which transcriptionally active DNA strands are repaired. This subpathway can most efficiently repair CPD lesions from transcribed strands of the gene (Spivak, 2015; Ura and Hayes, 2002; van Hoffen et al., 1995). In contrast, the GGR subpathway is independent of transcription and is able to remove DNA lesions from the entire genome, including both transcribed and non-transcribed regions. This leads to the GGR pathway being able to remove 6-4PPs most efficiently (Ura and Hayes, 2002). The biggest difference between the two pathways of the NER is the damage recognition step. In GGR the XPC complex (XPC-HR23B and CETN2 proteins) and Cul4-DDB complex (RBX1, Cul4, DDB1, and DDB2 proteins) are involved in DNA recognition, while TCR relies on RNA polymerase II and Cul4-CSA complex (RBX1, Cul4, DDB1, and CSA proteins) to recognize the damage (Spivak, 2015; Tornaletti and Hanawalt, 1999). Although these two pathways differ

slightly, their overall function remains the same: to remove DNA bulky adducts. The importance of the NER pathway can be demonstrated by the human diseases that result from genetic mutations in repair factors. At least three rare human autosomal recessive genetic disorders have been linked to mutations in the NER pathway: Xeroderma pigmentosum (XP), Cockayne syndrome (CS), and the photosensitive form of trichothiodystrophy (TTD) (Leibeling et al., 2006; van Steeg and Kraemer, 1999). All three diseases share some clinical symptoms including increased sun-sensitivity, freckling of the skin areas that have been exposed to sun, and a sharp increase in the rate of skin cancer incidents. To date, eight NER deficient XP complementation groups, two CS groups, and one TTD group have been identified, and in all cases the responsible genes have been cloned (Leibeling et al., 2006). Although the above three diseases are the most common NER deficient disorders, other DNA repair disorders are also known and include: Werner's syndrome (associated with premature ageing and retarded growth), Bloom's syndrome (sunlight hypersensitivity and high incidence of malignancies especially leukemias), and Ataxia telangiectasia (sensitivity to ionizing radiation and some chemical agents). All of the above mentioned diseases are often called "segmental progerias" (accelerated aging diseases), because the patients appear elderly and suffer from aging related diseases at an abnormally young age (Ellis, 1997; Friedbergy E.C. et al., 2006).

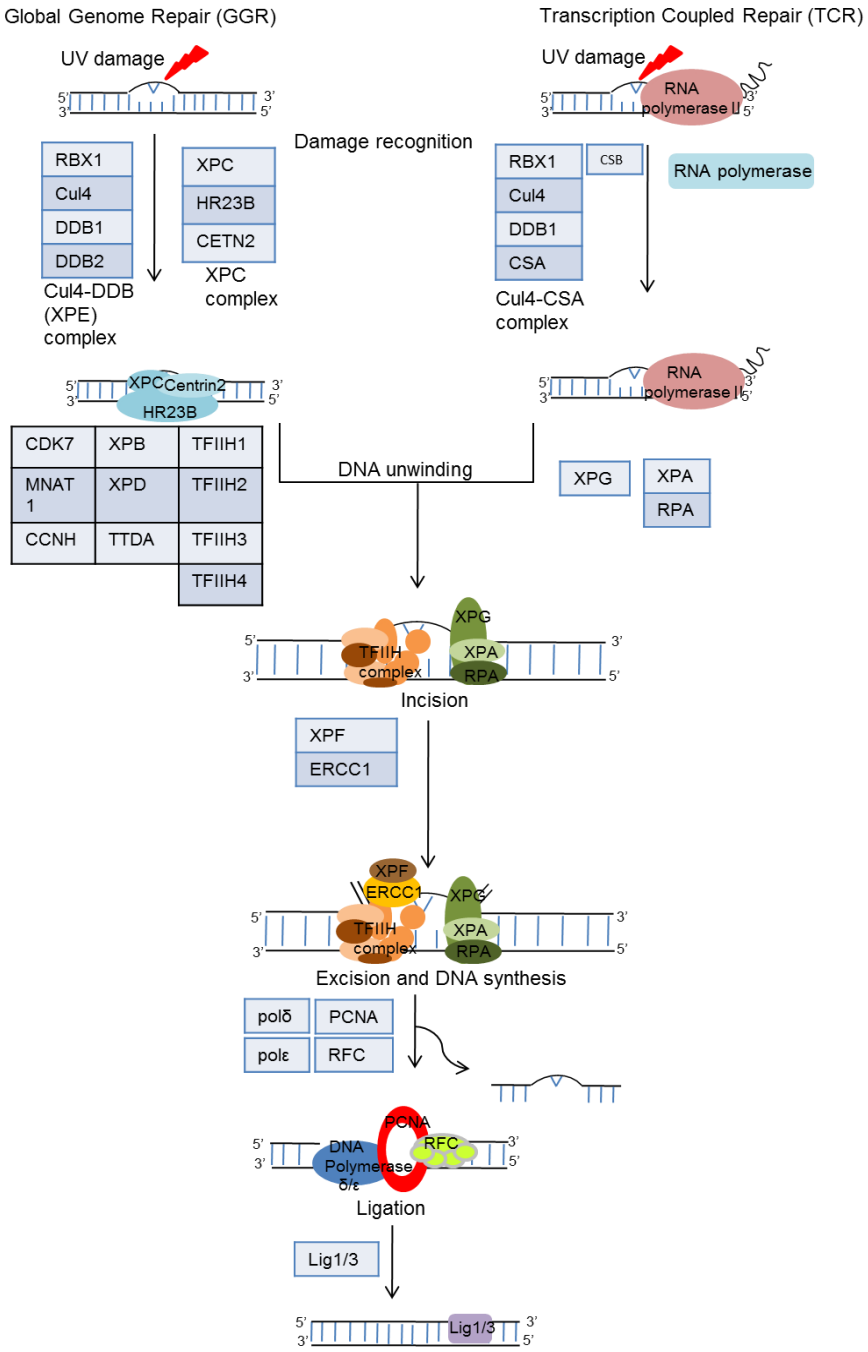

Figure 2: Nucleotide Excision Repair Pathway in Humans
The two subpathways of nucleotide excision repair in humans and the factors involved in both. Adapted from: Fousteri and Mullenders, 2008

Chromatin

In addition to the “classical” NER pathway factors there are several other players involved in DNA repair as well. One important player is chromatin. The chromatin plays an important role in many DNA-mediated functions including transcription, replication, and repair (Aydin et al., 2014; Ehrenhofer-Murray, 2004). In eukaryotic cells DNA is packaged into chromatin which includes histones and other non-histone proteins. The chromatin includes several increasingly compacted organizational forms of the DNA in the nucleus. The basic unit of chromatin is the nucleosome. Nucleosomal core particles are composed of 146 base pairs of DNA wrapped around a histone octamer which consists of two of each of the four core histones (H2A, H2B, H3, H4) (Ehrenhofer-Murray, 2004; Luger et al., 1997). Following incorporation of linker histone H1, nucleosomal arrays along the DNA fold into a 30 nm fiber (Figure 3). In cells that are non-dividing there are two types of chromatin present, euchromatin and heterochromatin. Euchromatin is uncompacted actively transcribed DNA and heterochromatin is compacted untranscribed DNA (Watson J.D. et al., 2014; Yu et al., 2005).

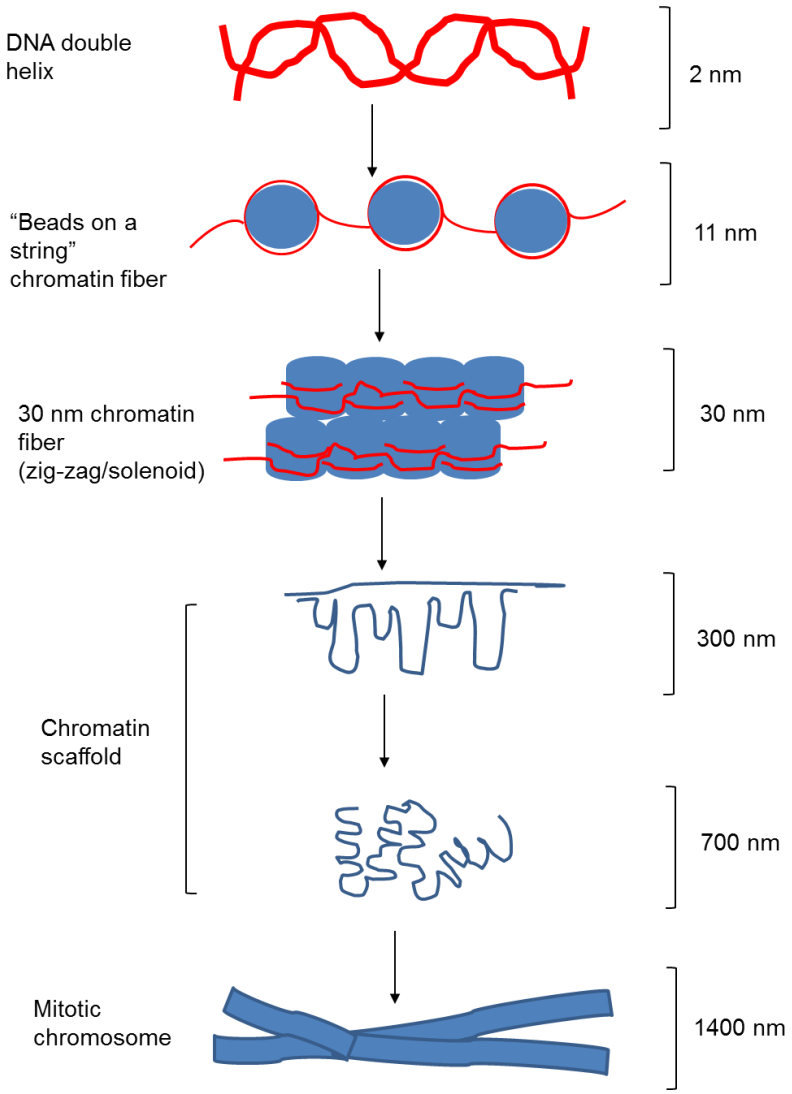

Figure 3: Levels of Chromatin Compaction in the Human Genome
The compaction of DNA into chromatin from 2 nm fiber to 1400 nm mitotic chromosome. The red color represents the DNA and the blue represents the proteinaceous part of the chromatin. Adapted from: Felsenfeld and Groudine, 2003

In eukaryotic cells, the inheritance of both the DNA sequence and its organization into chromatin is critical for maintaining genome stability and this maintenance is challenged when DNA damage occurs. Whenever damage occurs to the DNA, remodeling and unfolding of the chromatin is necessary to allow access to the DNA repair complexes. The first experiment that suggested that the structure of chromatin is rearranged during NER was an observation that nuclease accessibility to the DNA was modulated during UV induced DNA synthesis in IMR-90 human diploid fibroblasts (Smerdon and Lieberman, 1978). Studies have also shown that the ability of the cell to repair DNA damage is significantly reduced on UV damaged DNA pre-assembled into nucleosomes as compared to naked DNA and it was demonstrated that chromatin structure is altered during NER repair of UV induced DNA lesions (Adam and Polo, 2012; Green and Almouzni, 2002; Marteijn et al., 2014; Smerdon and Lieberman, 1978). As mentioned earlier, CPDs and 6-4PPs are the two most common classes of DNA lesions produced by UV irradiation. The distribution of these lesions is nucleotide sequence dependent, meaning the photoproducts tend to form on DNA strands that are able to easily unwind and bend to form the photoproducts, and the repair of the photoproducts is dependent several factors including transcription status and accessibility of repair machinery (Pfeifer, 1997). Several studies used reconstituted nucleosomes to study the effects of the nucleosome structure on the formation of UV induced DNA lesions (Green and Almouzni, 2002). One study used dinucleosomes to show

that the excision of 6-4PPs is strongly inhibited by chromatin structure even when the lesion is located in the linker DNA (Ura et al., 2001). Another study showed that the binding affinities of XPA and XPC for DNA are decreased as much as 5-fold on nucleosomal DNA as compared to naked DNA. This is significant as it is known that both proteins are required before excision of the damaged DNA can occur (Hara et al., 2000; Volker et al., 2001). These studies reiterate the importance of nucleosomal organization and also suggest that the compacted structure of the chromatin may restrict the path of repair proteins to the DNA lesions. These results suggest the theory that there may be additional cellular factors required to overcome the barriers that chromatin present for the NER pathway to function properly (Friedbergy E.C. et al., 2006; Gaillard et al., 1997).

Chromatin Remodelers

ATP-dependent chromatin remodelers are one of the factors that play an important role in the accessibility of the NER machinery to DNA damage sites in the nucleosomes. To date, more than 10 protein complexes have been purified that either disrupt or alter the association of DNA with histones (Aydin et al., 2014; Lai et al., 2013; Yodh, 2013). SWI/SNF chromatin remodeling enzymes are multi-subunit complexes that function by altering the chromatin structure thereby facilitating the binding of various regulatory proteins to the chromatin (Ura and Hayes, 2002). Each of these protein complexes contain an ATPase subunit of the SNF2 superfamily and fall into one of the three remodeling complex families:

SWI/SNF2-like, ISWI-like, and Mi-2-like (Friedbergy E.C. et al., 2006; Ura et al., 2001). Using reconstituted dinucleosomes, the effect of chromatin compaction on the formation of DNA lesions was studied. This study revealed that recombinant ACF (ATP-utilizing chromatin assembly and remodeling factor), and ATP (adenosine triphosphate)-dependent chromatin remodeling factor, facilitated the initiating steps of NER, specifically for the excision of 6-4PP lesions (Fei et al., 2011; Ura and Hayes, 2002).

Core Histones

Another mechanism that plays a role in the accessibility of the NER machinery to DNA damage sites is UV-induced core histone modifications. These post-translational histone modifications function as epigenetic switches between different chromatin states by modifying the N-terminal tails of histones via acetylation, phosphorylation, methylation, ubiquitination, and other post-translational modifications. These modifications direct several different cellular processes such as transcription, replication, DNA repair, and apoptosis (Soria et al., 2012; Trievel, 2004). Rogakou and colleagues were one of the first groups to discover the importance of post-translational histone modifications following DNA damage. They observed that the phosphorylation of a H2A variant, H2A.X, was one of the earliest events in response to double stranded DNA breaks (Rogakou et al., 1998). This finding gave insight into the importance of histone variants and post-translational modifications following DNA damage. Other studies have also

shown the importance of histone H2B phosphorylation and ubiquitylation, histone H3 and histone H4 acetylation and methylation, and histone H4 phosphorylation in double stranded break repair (van Attikum and Gasser, 2005).

Histone acetyltransferases (HATs) are a group of enzymes that are involved in chromatin unfolding. Addition of an acetyl group to the core histones n-terminal tails by the HATs neutralizes their positive charge, thus alleviating the strong interaction between the negatively charged DNA and the less positively charged histones (Friedbergy E.C. et al., 2006; Gray and Teh, 2001).

Yeast studies have shown that UV irradiation stimulates the acetylation of histones H3 and H4 at the repressed yeast locus *MFA2*. This acetylation occurs in the presence of Swi2p (an ATP-dependent chromatin remodeling complex) and GCN5, a known HAT. The study also showed that the absence of GNC5 resulted in no acetylation, which in turn resulted in impaired DNA damage repair (Yu et al., 2005). In another study, hyperacetylated mononucleosomes were shown to have enhanced repair synthesis 30 minutes after being exposed to UV irradiation in human fibroblast cells (Ramanathan and Smerdon, 1989). These results suggest that histone acetylation may increase the accessibility of repair enzymes to DNA damage. Another HAT protein, p300, was found to not only be linked with NER, but also with various other DNA repair mechanisms. p300 is known to be associated with recently synthesized DNA following UV irradiation possibly through its interaction with PCNA (proliferating cell nuclear antigen), a protein that

is key in DNA synthesis (Hasan et al., 2001). In addition to PCNA, p300 has also been associated with and known to acetylate several other non-histone proteins including: p53, BRCA1, NEIL 2, and many others (Bhakat et al., 2004; Grossman, 2001; Pao et al., 2000)

Histone deacetylases (HDACs) reverse the activity of HATs by removing the acetyl groups from core histones. Some published work suggested that deacetylation is important for the repair of DNA damage. One study showed the importance of the deacetylase complex Sin3p/Rpd3p for efficient repair of DNA damage caused by double-strand breaks in yeast (Fernandez-Capetillo and Nussenzweig, 2004). Another study found that in human cells, both HDAC1 and HDAC2 are found to be participants in double-strand break repair (Miller et al., 2010).

Phosphorylation of histones can also play a role in DNA repair. γ-H2AX, a histone variant, was the first histone modification found to be associated specifically with double stranded breaks in damaged DNA (Pilch et al., 2003). Methylation of histones is yet another modification that can lead to compaction of the chromatin and plays a role in transcriptional gene silencing. Scientists believed that DNA was only methylated and not demethylated until *LSD1* was classified as a demethylase (Kapoor et al., 2005; Szyf, 2005). Ubiquitination of histones plays an important role in several cellular processes including metabolic homeostasis, stress response, cell cycle regulation, and DNA repair. Studies showed that

ubiquitylation of histones H3 and H4 by CUL4-DDB-ROC1 is important for cellular response to DNA damage. A decrease in ubiquitylation of histone H3 and H4 following knockdown of CUL4A resulted in impaired recruitment of the XPC repair protein to DNA damage, resulting in the inhibition of NER (Wang et al., 2006).

High Mobility Group Chromatin Binding Proteins (HMGs)

The HMG proteins are among the largest and best characterized class of non-histone chromosomal proteins (Bustin and Reeves, 1996). There are three families of HMG proteins that are classified according to their functional DNA interaction motifs: HMGA, HMGB, and HMGN. The HMGA proteins contain an AT hook binding domain (which binds to the minor groove of adenine-thymine rich DNA), HMGB proteins contain a HMG-box binding domain, and the HMGN proteins contain a nucleosomal binding domain (Bustin and Reeves, 1996; Reeves, 2015). Each of these families are essential and highly dynamic constituents that play a role in different aspects of chromatin structure and function including DNA repair. HMGA proteins have been shown to preferentially bind to UV induced CPD photoproducts in stretches of AT-rich DNA, thereby inhibiting NER, while HMGB proteins have been shown to selectively bind to cisplatin-induced DNA cross-links and inhibit NER (Adair et al., 2005; Reeves and Adair, 2005). These results suggest that these two HMG families may be involved in the accumulation of mutations and chromosomal instabilities frequently observed in cancers. The HMGN family is composed of 5 proteins: HMGN1, HMGN2, HMGN3,

HMGN4, and HMGN5 (Kugler et al., 2012). HMGNs support accessibility to the nucleosomes by interacting with histone tails, competing with linker histone H1, and by regulating different post-translational modifications of core histones, all of which reduce the compaction of the chromatin fiber (Gerlitz, 2010; Lim et al., 2005; Postnikov et al., 2006).

HMGNS in NER

HMGN1 and HMGN2 are two ubiquitous members of the HMGN family that unfold chromatin to enhance transcription, replication, and repair processes in humans (Birger et al., 2003). When HMGN1 and HMGN2 proteins expression in the cell is disrupted, an increased sensitivity to UV irradiation, gamma irradiation, and heat shock was observed (Belova et al., 2008; Birger et al., 2005; Birger et al., 2003; Subramanian et al., 2009). Fousteri et al showed that HMGN1 is associated with Cockayne syndrome A protein in the TC-NER subpathway (Fousteri et al., 2006). Studies showed that HMGN1 knockout mice are more sensitive to UV irradiation and have a lower capacity to repair DNA damage (Birger et al., 2005). It has also been shown that Hmgn1 -/- fibroblasts have an altered G2-M checkpoint activation and are hypersensitive to ionizing radiation (Birger et al., 2005). These findings raise the hypothesis that HMGN1 is needed to unfold the chromatin structure and enable the accessibility of DNA repair machinery. Because the above experiments were performed with mice they did not include any information about the GGR subpathway, as mice lack efficient GGR. Alternatively, chicken

cells are similar to human cells in that they have efficient GGR. Research performed by Subramanian et al showed that UV irradiation of chicken lymphoblast cells lacking HMGN1, HMGN2, or both HMGN1 and HMGN2 have increased sensitivity to UV irradiation (Subramanian et al., 2009). In addition, it was shown that irradiated chicken lymphoblast cell lines disrupted for both HMGN1 and HMGN2 have a slower removal of CPDs as compared to wild type chicken lymphoblast cells (Subramanian et al., 2009). Together these results suggest that HMGN1 as well as HMGN2 are not only regulators of the TC-NER subpathway, but the GG-NER subpathway as well.

Possible Enhancements of NER

The nucleotide excision repair pathway is one of great importance and is critical for repair of UV damage. As mentioned earlier, any mutation or absence of any part of this pathway can lead to serious genetic disorders including xeroderma pigmentosum and Cockayne's syndrome. Therefore, not only is it imperative to have a functioning NER, but any enhancements in efficiency can be of great medical significance. Studies have suggested that the presence of certain players in NER could possibly enhance the repair efficiency (Chang et al., 1999; Choi et al., 2015; Yu et al., 2013). In yeast, DNA photolyase and the RAD proteins could be two possible factors involved in NER enhancement. DNA photolyases are pyrimidine-dimer repair enzymes that are activated by visible light. They contain two chromophore cofactors, one of which is a catalytic cofactor that directly

contributes to the repair of pyrimidine-dimers (Komori et al., 2001; Richa et al., 2015). *In vitro* experiments showed that the stimulation of excision repair by photolyases is a general phenomenon and that in addition to playing role in light-dependent repair, photolyases must also be considered an accessory protein in the NER pathway (Sancar and Smith, 1989). Unfortunately, the photolyase enzyme is not found in humans. Another yeast study suggested several RAD genes essential for NER. They suggested that the yeast RAD23 represents a class of accessory NER proteins and in the absence of these proteins NER activity is reduced (Xie et al., 2004). In humans, there are also several players that could lead to an enhancement of the NER pathway. One possibility is the tumor suppressor protein p53. This protein is necessary for this cell checkpoint and is only activated in stressful situations, such as ultraviolet or γ irradiation, heat, or low oxygen; therefore, it could serve as a possible enhancement tool for NER. However, studies have shown that sensitivity to damaged DNA is not enhanced in p53-negative cells (Friedbergy E.C. et al., 2006). Another study however, gave more promising results. These experiments used emodin (1,3,8-trihydroxy-6-methylanthraquinone), which is an active constituent of *Rheum palmatum* herb that has been shown to possess anticancer, antibacterial, diuretic, and vasorelaxant effects. Chang et al. looked at its role on NER and its influence on the repair of UV- and cisplatin-induced DNA damage in human fibroblast cells. Emodin increased unscheduled DNA synthesis (UDS) of UV-treated cells and reduced

cisplatin-induced DNA adducts in a concentration-dependent manner, indicating that emodin might promote NER capability in cells (Chang et al., 1999). Another possible mechanism for enhancing the NER pathway is the introduction of DNA repair enzymes via liposomes. Yarosh and colleagues showed that the addition of T4 endonuclease 5 via liposomes significantly reduced the rate of actinic keratosis and skin cancer in patients with XP (Yarosh, 2004).

Our research focus is the HMGN proteins and their possible role in the enhancement of the NER pathway. As mentioned earlier, in the absence of these proteins increased UV sensitivity and enhanced tumor burden is seen in knockout mice cells (Birger et al., 2003). Also, in chicken lymphoblast cells increased sensitivity to UV irradiation was seen in the absence of HMGN1a, HMGN2, or both HMGN1a and HMGN2 (Subramanian et al., 2009). This information coupled with the role of HMGNs in unfolding of the chromatin and DNA repair lead to my research hypothesis that cells overexpressing HMGNs will be less sensitive to UV irradiation. Our goal was therefore, to determine the effect the overexpression of HMGN proteins in human cells survival and DNA repair rates in response to UV irradiation and to also better understand HMGNs role in GG-NER.

Overexpression of HMGN Protein in Human HeLa Cells

To test the hypothesis that overexpression of the HMGN proteins leads to enhanced cell survival rate, human HeLa cells overexpressing HMGN1 (HeLa HMGN1-tag), human HeLa cells overexpressing HMGN2 (HeLa HMGN2-tag), and HeLa cells expressing basal levels of HMGN1 and HMGN2 (HeLa-tag) as a negative control were used. (a gift from Dr. Bustin, NIH, NCI). HeLa cells stably expressing either HMGN1-HA-FLAG or HMGN2-HA-FLAG tagged were established via the following means. HeLa cells were transduced with a retroviral construct containing an overexpression of HMGN1 or HMGN2 fused to a HA tag, FLAG tag, and an IL-2 receptor gene (Lim et al., 2002). Using immunomagnetic sorting, these cells were selected for stable transductants. As a control the HeLa cells were transduced only with a mock retroviral construct containing all the elements but the HMGN1/HMGN2 gene, these variants were named HeLa-tag (Figure 4).

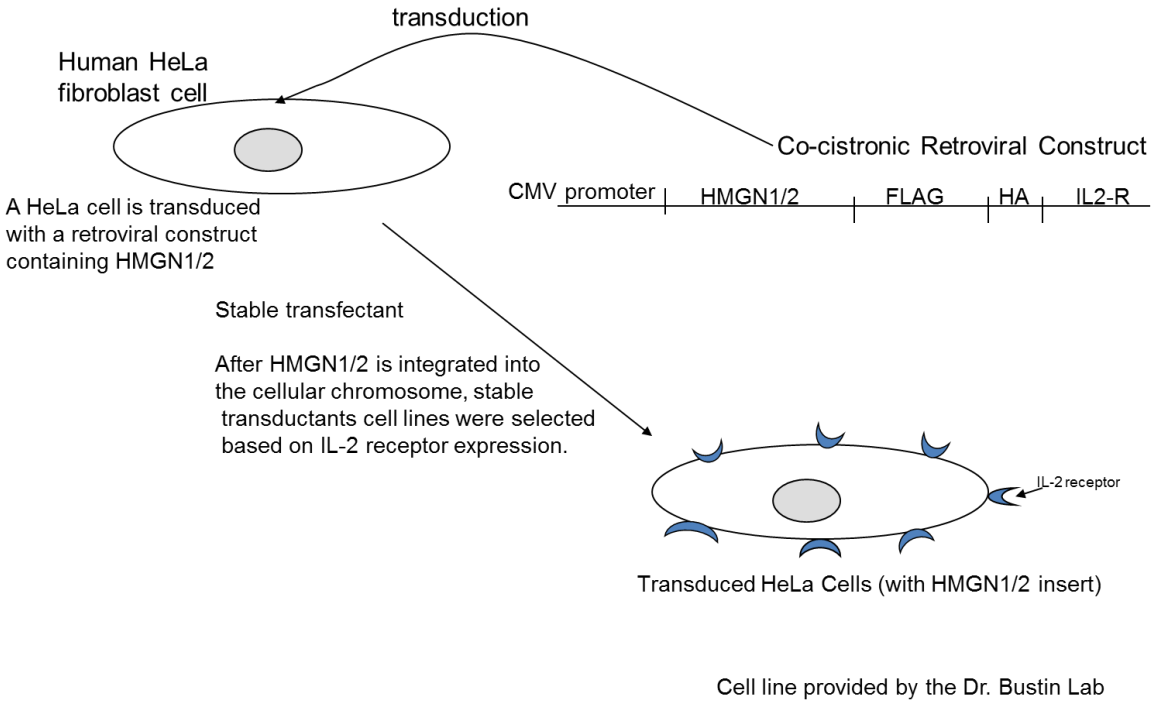

Figure 4: Derivation of HMGN1 and HMGN2 HA-FLAG Tagged Overexpressing Human HeLa Cell Lines

The establishment of cells lines containing either HMGN1-HA-FLAG or HMGN2-HA-FLAG tagged overexpressing cells. Each of these constructs were also fused to the IL2-R gene that served as a selectable marker. Cell line provided by Dr. Michael Bustin's lab.

CHAPTER II

MATERIALS & METHODS

Maintenance of Human HeLa HMGN Tag Cell Lines

HeLa overexpressing HMGN1 (HeLa HMGN1-tag), HeLa overexpressing HMGN2 (HeLa HMGN2-tag), and HeLa S3 (HeLa-tag) cells cell lines were maintained in Dulbecco's Modified Eagle's Medium (DMEM) (Gibco/BRL, #10566-016), supplemented with 10% fetal bovine serum (Benchmark, #100-106) and 1% penicillin-streptomycin (Gibco/BRL, #15140-122). Cells were grown in an incubator at 37˚C, 100% humidity and 5% CO_2.

UV Survival Assay

Exponentially growing HeLa-tag cells, HeLa HMGN1-tag cells, and HeLa HMGN2-tag cells with a concentration of 2 x 10^6 cells/ml were plated in 60 mm petri dishes and incubated at 37°C, 100% humidity and 5% CO_2 for 48 hours until 80% confluency was reached. The cells were washed with sterile 1X PBS (Cellgro, #21-040-CV), placed on ice, and irradiated with UVC (254 nm) at various joulages – 0, 10, 20, 30 J/m^2. The irradiated cells were incubated with fresh medium at 37˚C, 100% humidity and 5% CO_2 for 72 hours. Trypan blueexclusion assay was used to test cell viability. Cells that were colorless were determined to be alive and cells which stained blue were determined to be dead.

Survival curves were plotted so that survival was expressed as percentage of survived versus untreated cells (0 J/m^2). All experiments were conducted in triplicate and were repeated at least three independent times. The results were analyzed by repeated measures ANOVA $p < 0.05$.

Growth Curve of HeLa Cells

Exponentially growing HeLa cells with a concentration of 0.04×10^6 cells/ml were plated in 15.6 mm 24 well plates (Costar, CLS3524). These cells were maintained at 37°C, 100% humidity and 5% CO_2 and counted using trypan blue exclusion assay every 24 hours. Eight counts were made for every time point on hemocytometer slide and the graph was plotted with concentration of cells (cells/ml) versus time (hours). Standard deviation was used to determine the statistical variation of the growth curve. The results were anazliyzed by non-parametric Mann-Whitney U test $p \leq 0.1$. All experiments were done in triplicate.

Southwestern Analysis of Photoproduct Levels

Following UVC (254 nm) irradiation (30 J/m^2), DNA was extracted from cells at various times (0-40 hours) using the phenol-chloroform purification method (Sambrook and Russell, 2006). The DNA was transferred to Hybond-N^+ membrane (Amersham Pharmacia, #RPN119B) using a Minifold-1 slot blot system (Schleider & Schuell) and then cross-linked by 15 minute incubation at 80°C in a vacuum oven. Using anti-cyclobutane pyrimidine dimer (CPD) monoclonal

antibody (a gift from Dr. Bustin, NIH, NCI) (0.2 µg/ml) and anti-6-4photoproducts (6-4PP) monoclonal antibody (a gift from Dr. Bustin, NIH, NCI) (0.2 µg/ml), the relative levels of photoproducts were assessed. The relative level of DNA loaded onto each blot was determined by staining with 0.5 µg/ml ethidium bromide. The CPD/DNA ratio was determined using spot densitometry of the CPD/6-4 PP blot by AlphaImager and Fluorchem HD2 software. The results were analyzed by Mann-Whitney U test, $p < 0.05$.

SDS-PAGE and Western Blot Analysis

Whole cell lysates from HeLa cells (irradiated and non-irradiated) were run on SDS-PAGE (sodium-dodecyl-sulphate polyacrylamide gel electrophoresis) in order to separate the proteins based on their molecular weight. Whole cell lysates were collected using 1X SDS buffer (100 mM Tris-CL, 4% SDS, 100 mM DTT, 20% glycerol, and cOmplete protease inhibitor tablet (Roche, #11836153001). The extracted lysate was boiled at 94°C for 20 minutes to denature DNA, centrifuged at 14,000 rpm for 30 seconds, and the protein concentration was measured using a detergent and reducing agent compatible – 660 nm Protein Assay Kit (Pierce, #22660, 22663). The cellular extracts were resolved on SDS-PAGE and equal loading was confirmed by Coomassie staining and densitometric analysis, using AlphaImager and Fluorchem HD2 software. Once equal protein loading was established, the proteins were transferred from the SDS-PAGE to a PVDF membrane (Millipore, #IPVH00010) at 28 mA for

2 hours using a trans-blot semi-dry transfer machine (Bio-Rad). Following transfer the membrane was blocked for 45 minutes in blocking buffer, PBS-Tween (1X PBS with 0.1% tween 20) containing 5% non-fat dry milk (Nestle carnation). After a rinse with 1X PBS, the membrane was incubated with a primary antibody against the protein of interest overnight at 4°C. The primary antibodies used in this work include: anti-HMG-14 (sc-19074, 0.001 µg/ml), anti-HDAC2 (sc-6296, 2 µg/ml), anti-HA (sc-805-G, 0.2 µg/ml), normal mouse IgG (sc-3878, 0.4µg/ml), goat anti-mouse IgG-FITC (sc-2010, 0.002 µg/ml), anti-actin (sc-56459, 0.08 µg/ml), anti-XPC (sc-74411, 0.2 µg/ml), anti-HDAC1 (sc-6299, 0.1 µg/ml), anti Ac-H4K5 (sc-8659, 0.08 µg/ml). Then, the membrane was subjected to one 10 minute wash followed by two 5 minute washes of PBS-Tween and incubated with horseradish peroxidase conjugated secondary antibody (Thermo Scientific) targeted against the primary antibody at room temperature for 1 hour. The secondary antibody used varied dependent upon which primary antibody was used, but included: rabbit anti-mouse IgG HRP (Pierce, #31450, 0.1 µg/ml), goat anti-rabbit IgG HRP (Thermo, #31460, 0.1 µg/ml), rabbit anti-goat IgG HRP (Thermo, #31402, 0.05 µg/ml), goat anti-mouse (Pierce, #31431, 0.1 µg/ml). The membrane was then again subjected to one 10 minute wash followed by two 5 minute washes of PBS-Tween and treated with ECL plus kit (Amersham Biosciences, # RPN2133) and exposed to x-ray film

(GE Healthcare, #28-9068-35). Densitometric analysis (Alpha Innotech) was performed to quantify the bands.

Histone Post-Translational Modifications in UV Irradiated Human HeLa Cells

HeLa-tag cells and HeLa HMGN1-tag cells were plated in 100 mm tissue culture plates (Sarstredt) and incubated at 37°C, 100% humidity and 5% CO_2 for 48 hours until 80% confluency was reached. These cells were UV irradiated at 30 J/m^2 (254 nm) and whole cell lysates were extracted at various times after UVC irradiation: 30 minutes, 4 hours, 10 hours, 24 hours, 48 hours, and 72 hours using 1X Laemmli buffer. Non-irradiated cells were used as a control. The proteins were resolved on a 15% SDS-PAGE and subjected to Western blot analysis (explained on page 23) using specific antibodies against acetylated H3K9 (Upstate, #06-942, 1 µg/ml), acetylated H3K14 (Upstate, # 06-911, 0.4 µg/ml), and acetylated H4K5 (SantaCruz Biotech, # sc-8659-R, 0.08 µg/ml). The protein loading was standardized using Coomassie staining technique of core histones. ECL treated membranes were exposed to X-Ray films (GE Healthsciences), and levels of acetylation were determined using spot densitometry by an AlphaImager and Fluorchem HD2 software. The percent acetylation levels were calculated based on three separate experiments. The results were analyzed by Kruskal-Wallis analysis of variance, $p < 0.05$.

Co-Immunoprecipitation Assay

Whole cell lysates were prepared using radio immunoprecipitation assay (RIPA) buffer (0.5% 500 µM NP40, 0.8% 0.5 M NaF, 2% 100 mM Na-Orthovanadate, cOmplete protease inhibitor tablet in 1X PBS). After 30 minutes of incubation at 4°C, cell lysates were passed through a 20 gauge syringe and centrifuged for 20 minutes at 10,000 g to collect supernatant to be used for immunoprecipitation. The protein concentration was then determined by Micro BCA Protein Assay Kit (Thermo Scientific, #23235). The whole cell lysate (1-2 mg protein concentration) was pre-cleared with 0.25 µg/ml of non-immune IgG, either normal mouse, rabbit, or goat IgG (Santa Cruz Biotechnology, #sc-2025, #sc-2027, and #sc-2028) corresponding to the host species of the primary antibody and 20 µl of protein-A/G agarose conjugate per ml (Santa Cruz Biotechnology, #sc-2003). This solution was placed on a rotary shaker at low speed and 4°C for 1 hour. After preclearing, the supernatant was collected by centrifugation at 2,500 rpm for 5 minutes at 4°C. Either anti-HMGN1 antibody (Santa Cruz Biotechnology, #sc-19074, 0.001 µg/ml), anti-HDAC2 antibody (Santa Cruz Biotechnology, #sc-6296, 2 µg/ml), or anti-HDAC1 antibody (Santa Cruz Biotechnology, #sc-6299, 0.1 µg/ml) was added to the supernatant. A negative control was prepared by immunoprecipitating the whole cell lysates using non-immune IgG antibodies. Following an overnight incubation at 4°C on a rotator, the pellet was collected by centrifugation at 2,500 rpm for 5 minutes at 4°C. Following three washes with RIPA buffer and centrifugation, 30 µl of 1X SDS Laemmli loading buffer was added

to the pellet and each sample was boiled for 5 minutes at 94°C. These samples were subjected to 10% or 15% SDS-PAGE and Western blot analyses (explained on page 23) were performed to detect the protein bound to the immunoprecipitated protein.

Pull-Down Assay

Recombinant human HMGN1 (a gift from Dr. Bustin, NIH, NCI), recombinant full length human rhp300 protein (Active Motif, #31205), or recombinant full length human HDAC2 (rhHDAC2) protein (Enzo life sciences, # BML-SE533-0050) were used. Equal µg's of HMGN1 with p300 or HDAC2 were added and allowed to interact at 4°C on rocker for 1 hour. Following incubation either: anti-HMGN1 (Bethyl laboratories, #A302-362A, 0.05µg/1µl), anti-p300 (Santa Cruz Biotechnology, #sc-585, 1µg/1µl), or anti-HDAC2 (Santa Cruz Biotech, #sc-6296, 2 µg/ml) were added and allowed to interact with recombinant proteins 4°C on rocker for 1 hour. Protein A/G-agarose beads were added last, and pull-down was carried out with an overnight incubation at 4°C on rocker. After overnight incubation, the pull-down reaction was subjected to centrifugation at 1,000 g for 5 minutes at 4°C and two washes the reaction was resuspended in 1X Laemmli buffer. Samples were run on a 10% or 15% SDS-PAGE and either stained with Coomassie blue or subjected to Western blot analysis.

Protein bands were analyzed by spot densitometry using Alpha Innotech and Fluorchem HD2 software.

Immunocyctochemistry

HeLa S3 cells were grown on glass coverslips (Gold seal, #3350) until 80% confluency was reached. Once confluency was reached cells were exposed to local UV irradiation (UVC, 254 nm, 100 J/m^2) through 3 µm isopore membrane filters (Millipore, #TSP01300) that were placed on the cells, or left as a non-irradiated control. Then the cells were placed back in the incubator (at 37°C, 100% humidity and 5% CO_2) until indicated times (range from 30 minutes – 24 hours), washed with 1X PBS and fixed with 4% para-formaldehyde (Fisher) for 10 minutes. Following fixation cells were permeabilized and blocked with TNBS buffer (0.1 % triton x-100, 1% FBS, 0.1% NaN3 in 1X PBS) or BSA buffer (1% bovine serum albumin in 1X PBS) for 30 minutes and then incubated with antibody against protein of interest overnight at 4°C. Negative controls for all experiments were performed using non-immune IgG of the same species as the experimental group's primary antibody. After overnight incubation and three 10 minute washes with 1X PBS, cells were incubated with secondary antibody (Santa Cruz Biotech) conjugated to a fluorescent tag for 75 minutes at room temperature. The cells were then subjected to three 10 minute washes with 1X PBS, and counterstained with Hoechst (Invitrogen, #62249) for 5 minutes to stain the DNA. The coverslips were mounted on microscope slides with prolong antifade mounting medium

(Invitrogen, #P36934) and allowed to dry overnight. The cells were viewed using a Nikon A1R Confocal Microscope and analyzed with NIS-Element C software.

Recombinant HMGN1 Construction

HMGN1-GFP (a gift from Dr. Bustin, NIH, NCI) was used to obtain recombinant HMGN1. Using PCR (94°C, 1 minute 30 seconds; 55°C, 1 minute 30 seconds; 72°C, 5 minutes, 25 total cycles) and custom made forward and reverse primers (Biolane Synthax, Forward primer sequence: TGAATTCATGCCCAAGAGGAAGGTCAGCTC and Reverse primer sequence: GGGATCCTTAATCAGACTTGGCTTCTTTCT) we isolated the HMGN1 gene cloned next to the GFP clone. Following the isolation, the HMGN1 gene was purified (QIAquick PCR purification kit, #28104, Qiagen) and a restriction digest of the HMGN1 gene and the pMAL vector, used for ligation, (gift from Dr. J. Knesesk, TWU) was performed. The restriction digest used the restriction enzymes, BamHI and EcoRI (New England Biolabs, #R0101S and #R0136S), both of which were located on the pMAL vector and HMGN1 gene. To confirm the restriction digest, 0.7% and 1.5% agarose gels (made with TBE buffer) were run. Once confirmed, a 3-fold molar excess of HMGN1 gene (insert) was combined with 50 ng of the pMAL vector, T4 DNA ligase and Quick ligation buffer. The solution was incubated for 5 minutes at room temperature, and then chilled on ice using a quick ligation kit (New England Biolabs, #M2200S). Following the ice chill, transformation of the ligated vector and insert was done with DH5α cells (New England Biolabs, #11319-

015) that were plated on LB+amp+X-gal+IPTG plates. The colonies that grew on the plates were screened and “positive” or white colonies (colonies that contain the plasmid with the ligated HMGN1 gene) had their DNA extracted using a Qiagen mini kit (Qiagen, #51304). Finally a PCR using the previously used forward and reverse primers for HMGN1 was performed and a 1.5% agarose gel was run to confirm that the colonies did in fact contain the gene of interest.

CHAPTER III

RESULTS

Overexpression of HMGN1 Protein in Human HeLa Cells

Previous studies have shown that mice lacking the HMGN1 gene were hypersensitive to UV and gamma irradiations and displayed a decreased DNA repair rate (Birger et al., 2003). Previous studies have shown that chicken lymphoblastoid cells (DT40) that have a deletion of the HMGN1a and HMGN2 genes also display hypersensitivity to UV irradiation and a decreased DNA repair rate (Subramanian et al., 2009). Thus, both studies suggest that the HMGN1 protein is involved in nucleotide excision repair (NER) pathway. Here we wanted to test the functional significance of overexpressing HMGN1 protein in a human cell system. The question we asked was would the overexpression of HMGN1 or HMGN2 in human HeLa cells increase the level of cell survival and nucleotide excision repair rate?

Control HeLa cells were transduced with a retroviral construct containing HMGN1 or HMGN2 fused to a HA tag, FLAG tag, and an IL-2 receptor under the regulation of the CMV promoter (Lim et al., 2002). Using immunomagnetic sorting, HMGN1/N2 overexpressing stable transductants were selected based on the expression of the IL-2 receptor on their membranes. As a control the HeLa cells were transduced only with a mock retroviral construct containing all the

elements, but the HMGN1/N2 gene, these variants were named HeLa-tag. Using Western blot (Figure 5), it was determined that the overexpressing cells, named HeLa HMGN1-tag (a gift from Dr. Bustin, NIH, NCI) contained approximately 50% more HMGN1 than control HeLa cells (numerically represented in Table 1).

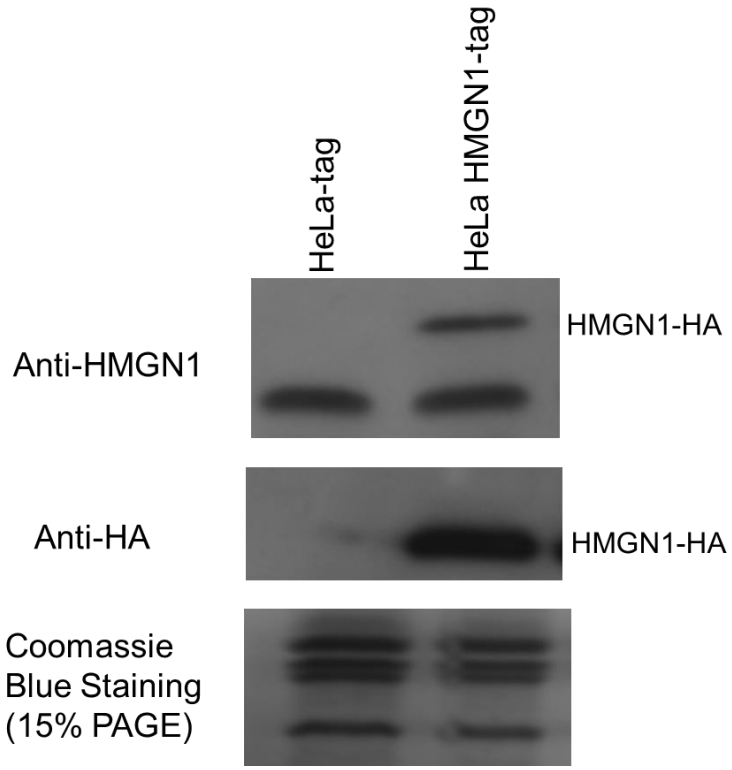

Figure 5: Western Blot Analysis of HeLa-tag and HeLa HMGN1-tag Cells to Determine HMGN1 Expression Levels
Western blot shows HeLa HMGN1-tag cells contain approximately 50% more HMGN1 than control HeLa cells (measured by HMGN1-HA band).

Table 1: Expression Levels of HMGN1-HA Protein in Stably Transfected HeLa Cells

Protein	HeLa-tag cells	HeLa HMGN1-tag cells
HMGN1	0.437	0.579
HMGN1-HA	0	0.381
TOTAL	0.437	0.96

A numerical representation of the expression levels of HMGN1 and HMGN1-HA based on the Western blots shown in Figure 5.

Overexpression of HMGN1 Protein Leads to Enhanced Cell Survival Rate

Control HeLa (HeLa-tag) and overexpressing HMGN1 HeLa (HeLa HMGN1-tag) cells were irradiated with UVC doses ranging from 1-30 J/m^2. Seventy-two hours following irradiation, the cell survival rate was measured by trypan blue exclusion assay and compared to the survival rate of non-irradiated cells. The HeLa HMGN1-tag cells demonstrated a significant hyposensitivity to UV as compared to the HeLa-tag control cells (Figure 6). This hyposensitivity shown across all joulages tested was in agreement with the higher sensitivity of the previously reported HMGN1/2 disrupted chicken cells and mice knockout cells (Birger et al., 2003; Subramanian et al., 2009).

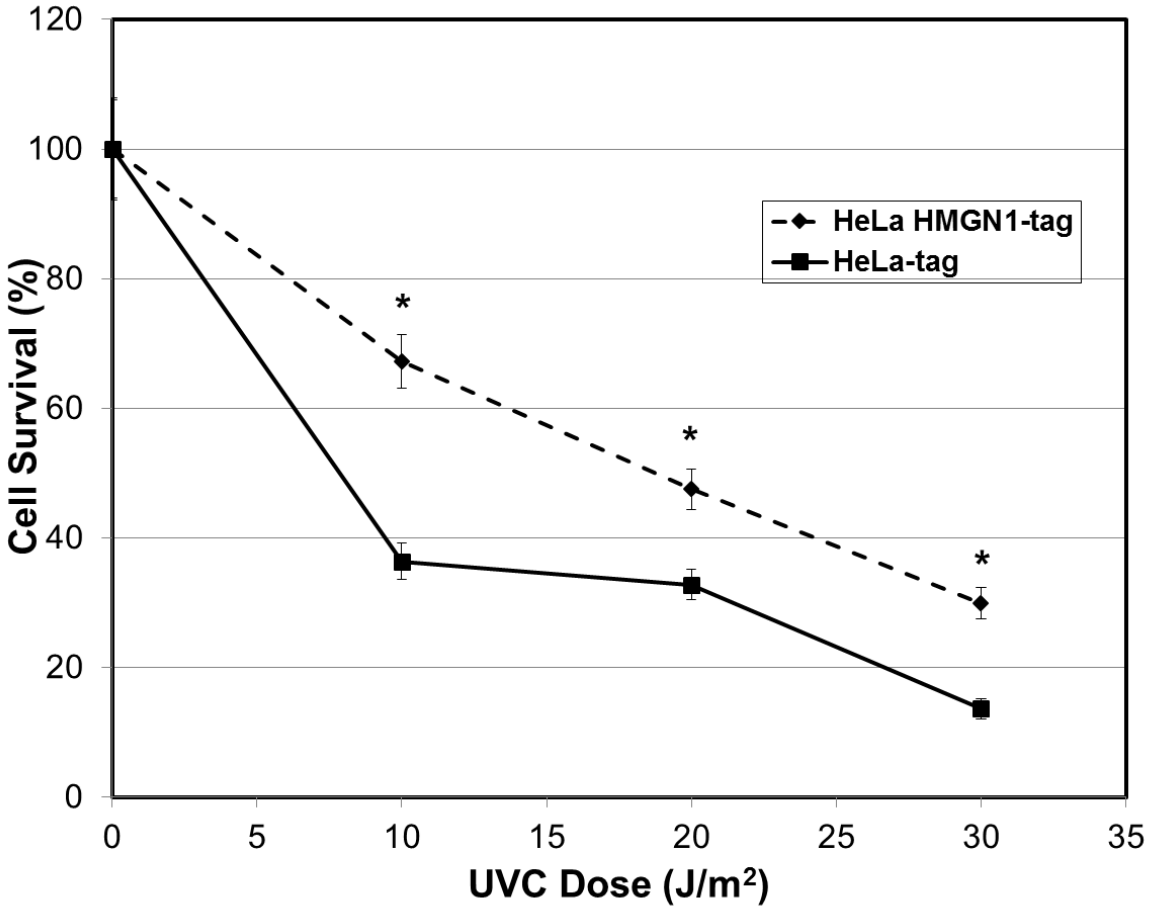

Figure 6: Overexpression of HMGN1 Leads to Enhanced UVC Survival
Shown are survival curves of HeLa-tag and HeLa HMGN1-tag cells 72 hours following UV irradiation, with doses of UVC ranging from 0-30 J/m^2. HeLa HMGN1-tag cells showed decreased sensitivity to UV irradiation. Each data point represents the mean of three independent measurements (± SE) as measured by trypan blue exclusion assay.
Note: * indicates significant difference in cell survival between HeLa HMGN1-tag cells and HeLa-tag cells as determined by repeated measures ANOVA test ($p \leq 0.05$).

HeLa HMGN2-tag Cells and HeLa-tag Cells Display Similar Sensitivity to UV Irradiation

As mentioned, previous studies have shown that chicken lymphoblastoid cells (DT40) that have a deletion of the HMGN1a and HMGN2 genes displayed hypersensitivity to UV irradiation and a decreased DNA repair rate (Subramanian et al., 2009). After demonstrating that cells overexpressing HMGN1 had an enhanced cell survival rate, we wanted to determine the effect of overexpressing HMGN2 protein on UV resistance. Using HMGN2 overexpressing HeLa cells (hereafter named HeLa HMGN2-tag cells) (a gift from Dr. Bustin, NIH, NCI), a cell UV-survival assay was performed. Control HeLa (HeLa-tag) and HMGN2 overexpressing HeLa (HeLa HMGN2-tag) cells were irradiated with UVC doses ranging from 0-30 J/m^2. Seventy-two hours following irradiation, the cell survival rate was measured by trypan blue exclusion assay. The HeLa HMGN2-tag cells demonstrated similar sensitivity to UV as compared to the HeLa-tag control cells (Figure 7). These results were in contrast to the lower UV sensitivity observed with HeLa HMGN1-tag cells suggesting that HMGN1 proteins levels could be a rate limiting step, while HMGN2 levels are not.

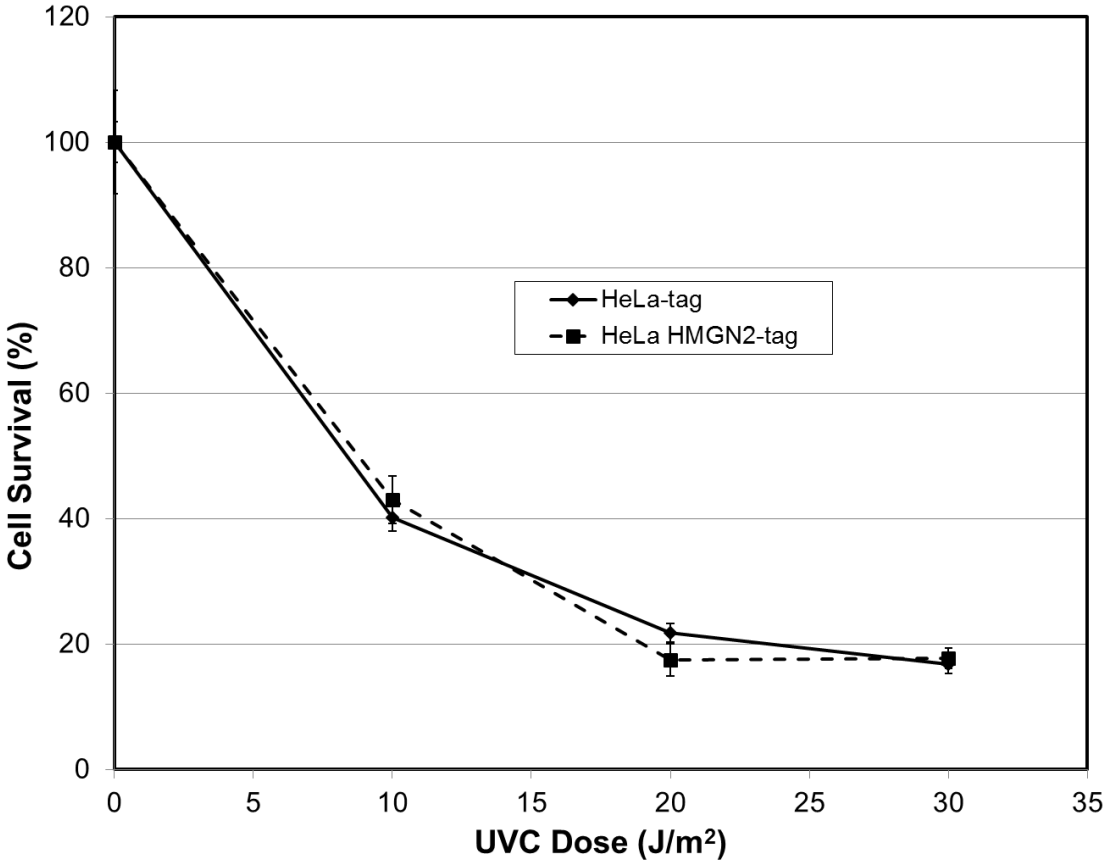

Figure 7: HeLa HMGN2-tag Cells and HeLa-tag Cells Display Similar Sensitivity to UV Irradiation

Shown are survival curves of HeLa-tag and HeLa HMGN2-tag cells 72 hours following UV irradiation, with doses of UVC ranging from 0-30 J/m^2. Each data point represents the mean of three independent measurements (± SE) as measured by trypan blue exclusion assay.

Note: HeLa HMGN2-tag cell survival was not significantly different from HeLa-tag cell survival as determined by repeated measures ANOVA ($p \geq 0.05$).

The LD_{50} values of UV irradiated HeLa-tag (control cells), HeLa HMGN1-tag, and HeLa HMGN2-tag cell lines are shown in Table 2. These numbers were calculated based on UV cell survival assay experiments and they corroborate the low UV sensitivity of HeLa HMGN1-tag cells and the control level UV sensitivity of HeLa HMGN2-tag cells.

Table 2: LD_{50} of UV Irradiated HeLa-tag, HeLa HMGN1-tag, and HeLa HMGN2-tag Cell Lines

HeLa-tag	HeLa HMGN1-tag	HeLa HMGN2-tag
7.8± 0.7 J/m^2	19.2 ± 3.9 J/m^2*****	8.7 ± 1.8 J/m^2

The LD_{50} values (in J/m^2 ± SE) of the HeLa-tag, HeLa HMGN1-tag, and HeLa HMGN2-tag cells were calculated based on the experiments shown in Figure 6 and Figure 7 (n=3). Note: * indicates significant difference of LD_{50} of HeLa HMGN1-tag cell versus HeLa-tag cell LD_{50} as determined by non-parametric Mann-Whitney U test ($p \leq 0.1$)

HeLa-tag and HeLa HMGN1-tag Cells Display a Similar Growth Pattern

To test whether the enhanced hyposensitivity following UV irradiation by HeLa HMGN1-tag cells was simply because the HeLa HMGN1-tag cells displayed a growth rate advantage over the HeLa-tag cells, the growth rates of HeLa-tag and HeLa HMGN1-tag cells were studied by a growth curve experiment. The results showed that there was no significant differences between the growth rate of either cell line as measured by their doubling time and saturation density (Figure 8 and Table 2).

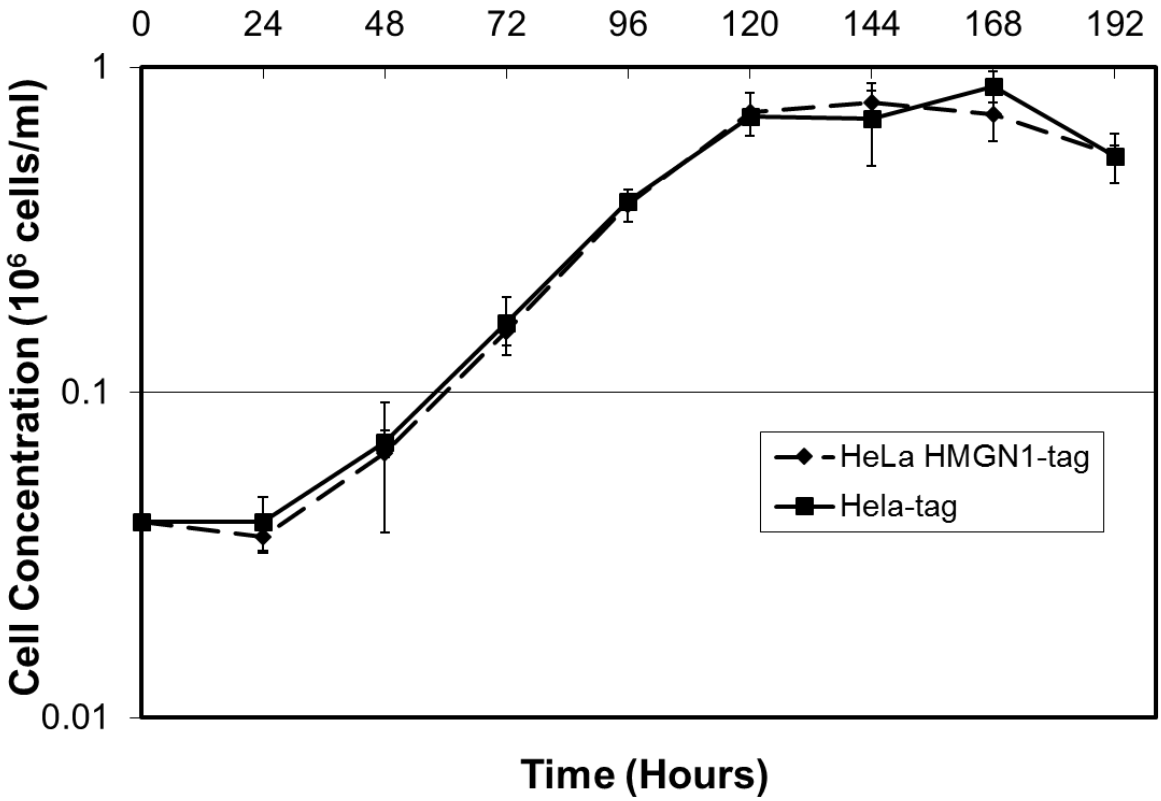

Figure 8: HeLa HMGN1-tag and HeLa-tag Cells Growth Curve
Growth curves of HeLa-tag and HeLa-HMGN1 tag cells. All points are the mean of three replicate plates with error bars indicating the standard error.

Because of this, we wanted to test other possible causes for the UV-hyposensitivity of HeLa HMGN1-tag cells. One option was that the HeLa HMGN1-tag cells repair their DNA damage at a faster rate than HeLa-tag cells.

Table 3: Saturation Density and Doubling Time of HeLa-tag and HeLa HMGN1-tag Cells Grown at 37°C

Cell Line	HeLa HMGN1-tag	HeLa-tag
Saturation Density ± SE (10^6 cells/ml)	0.82 ± 0.02	0.77 ± 0.07
Doubling Time (hours)	23.3 hours ± 2.8	23.3 hours ± 0.7

Numbers for the chart were calculated based on Figure 5, using three independent experiments. Saturation density is defined as the maximal concentration the cells reach. Doubling time is defined as the time it takes for the cells to duplicate their concentration at the logarithmic phase of the curve (i.e.: at their maximal growing rate).
Note: No significant differences in saturation density or doubling time between HeLa-tag and HeLa HMGN1-tag were seen as determined by non-parametric Mann-Whitney U test ($p \geq 0.1$).

HeLa HMGN1-tag Cells Display an Enhanced DNA Repair Rate

Next, experiments were performed that tested whether the reduced sensitivity of the HeLa HMGN1-tag cells was due to an enhanced DNA repair rate as compared to HeLa-tag cells. Using a Southwestern blotting (see Materials and Methods) we analyzed the kinetics of cyclobutane pyrimidine dimers (CPDs) and 6-4 Photoproducts (6-4PPs) removal rate from DNA in HeLa-tag and HeLa HMGN1-tag cells following UV irradiation. Subsequent to UV irradiation, a gradual decrease in the amount of CPD damage was seen. However, a significantly faster decrease of the CPDs in the HeLa HMGN1-tag cells at 10 hours after UV irradiation

as compared to the HeLa-tag cells (Figures 9 and 10) was observed. At 10 hours approximately 30% of the CPD adducts had been removed in the HeLa HMGN1-tag cells, while the HeLa-tag cells still showed a significant damage.

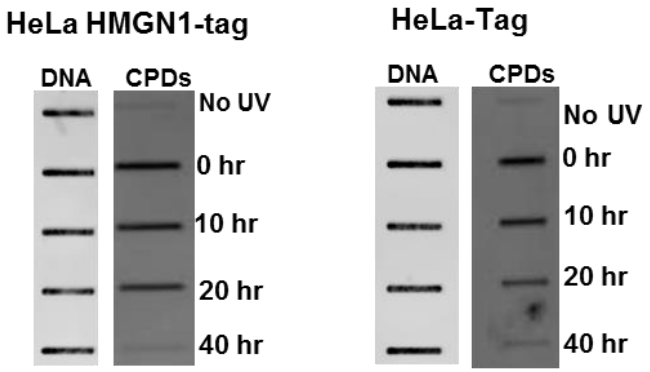

Figure 9: CPD Photoproduct Removal in HeLa HMGN1-tag and HeLa-tag Cells
Shown is Southwestern analysis of CPD removal in both HeLa-tag and HeLa HMGN1-tag cells. DNA was extracted at 0, 10, 20, and 40 hours following UVC irradiation with a dose of 30 J/m^2. DNA (2 µg for DNA control and 1 µg for CPDs) was loaded per slot in a Slot Blot system and transferred to Hybond-N$^+$ membrane. The membrane was incubated with CPD monoclonal antibody and the CPD values were normalized against DNA levels quantified by staining the membranes with EtBr. The CPD/DNA ratio was determined using spot densitometry.

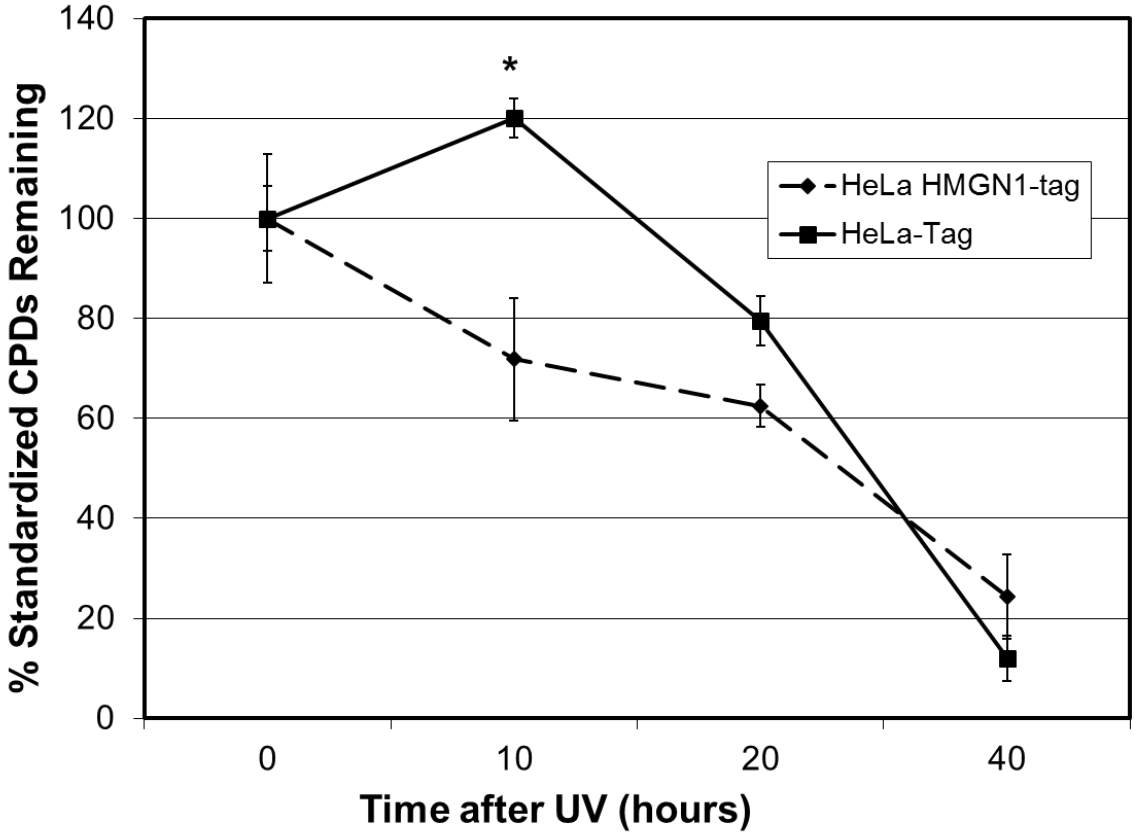

Figure 10: Enhanced CPD Repair Rate in HeLa HMGN1-tag and HeLa-tag Cells
Quantification of the experiment represented in Figure 9. The line graph represents the kinetics of removal of CPD photoproducts. The percent standardized CPDs remaining is the percentage of CPD levels at the time interval following UV irradiation relative to the levels of CPDs immediately after UV irradiation (0 hr). The graph represents the means (± SE) from three independent experiments.
Note: Significant difference of CPD concentration of HeLa-tag versus HeLa HMGN1-tag is indicated by * as determined by non-parametric Mann-Whitney U test, ($p \leq 0.05$).

The 6-4PP's levels also displayed a gradual decrease following UV irradiation, with significantly less lesions in HeLa HMGN1-tag as compared to HeLa-tag cells detected 4 hours post irradiation (Figures 11 and 12). These results indicated that HeLa HMGN1-tag cells have an enhanced nucleotide excision repair capacity as compared to HeLa-tag cells. Thus, HeLa HMGN1-tag cells hyposensitivity to UV irradiation may be explained by their higher capacity to remove UV-induced DNA lesions.

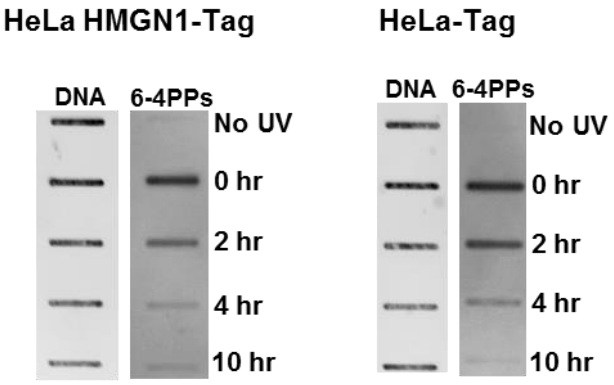

Figure 11: 6-4PP Photoproduct Removal in HeLa HMGN1-tag and HeLa-tag Cells
Shown is Southwestern analysis of 6-4PP removal in both HeLa-tag and HeLa HMGN1-tag cells. DNA was extracted at 0, 2, 4, and 10 hours following UVC irradiation with a dose of 30 J/m^2. DNA (2 µg for DNA control and 1 µg for 6-4PPs) was loaded per slot in a Slot Blot system and transferred to Hybond-N^+ membrane. The membrane was incubated with 6-4PP monoclonal antibody and the 6-4PP values were normalized against DNA levels quantified by staining the membranes with EtBr. The 6-4PP/DNA ratio was determined using spot densitometry.

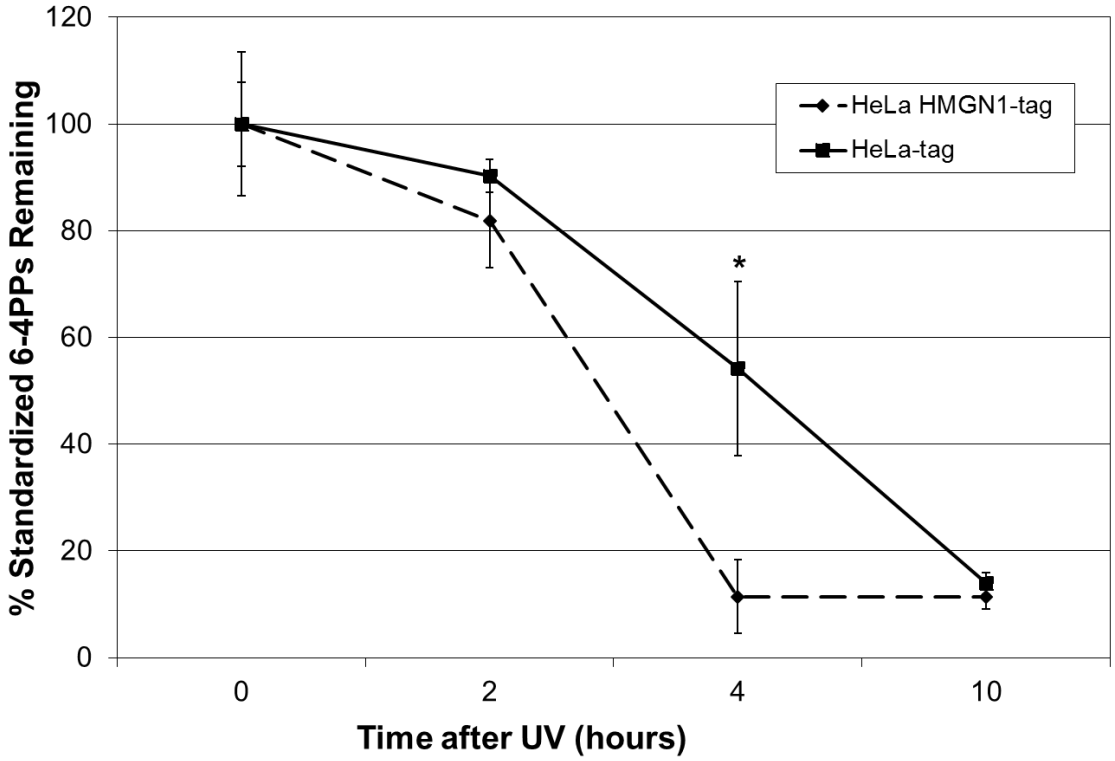

Figure 12: Enhanced 6-4PP Repair Rate in HeLa HMGN1-tag and HeLa-tag Cells
Quantification of the experiment represented in Figure 11. The line graph represents the kinetics of removal of 6-4PP photoproducts. The percent standardized 6-4PPs remaining is the percentage of 6-4PP levels at the time interval following UVC irradiation relative to the levels of 6-4PPs immediately after UV irradiation (0 hr). The graph represents the means (± SE) from three independent experiments.
Note: Significant difference of 6-4PP concentration of HeLa-tag versus HeLa HMGN1-tag is indicated by * as determined by non-parametric Mann-Whitney U test, ($p \leq 0.05$).

Previous Southwestern studies performed in the lab, using chicken knockout cell lines, showed that the loss of HMGN1 resulted in a decreased removal rate of CPDs (Subramanian et al., 2009). Also, it has been shown that the loss of HMGN1 protein in MEF (mouse embryonic fibroblast) cells leads to a decreased DNA repair rate (Birger et al., 2003). Combined, these results suggested that HMGNs affect the repair rate of UV induced DNA lesions in several vertebrate species from avian to humans. These results could explain the lower death rate of HMGN1 overexpressing HeLa cells following UV irradiation. Thus, if overexpression of HMGN1 in HeLa cells contributes to a more efficient removal of CPDs & 6-4PPs from DNA, the cells have a higher survival rate.

Starting CPD/DNA Ratio After UV Irradiation in HeLa-tag and HeLa HMGN1-tag Cells

We wanted to test whether HeLa HMGN1-tag cells appeared to have an enhanced DNA repair rate because they started with lower DNA photoproduct to DNA levels (less damage) or that the starting damage rate was similar, and actually the repair was more efficient. We therefore analyzed both the CPD/DNA and 6-4PP/DNA ratio immediately following UV irradiation (time zero) in both cell lines and determined that there are no statistically significant differences in DNA damage between the HeLa HMGN1-tag and the HeLa-tag cell lines (Figure 13). These findings support the conclusion that HMGNs affect the rate of repair for UV

induced DNA damage and not the initial rate of UV induced DNA photoproducts (Subramanian et al., 2009).

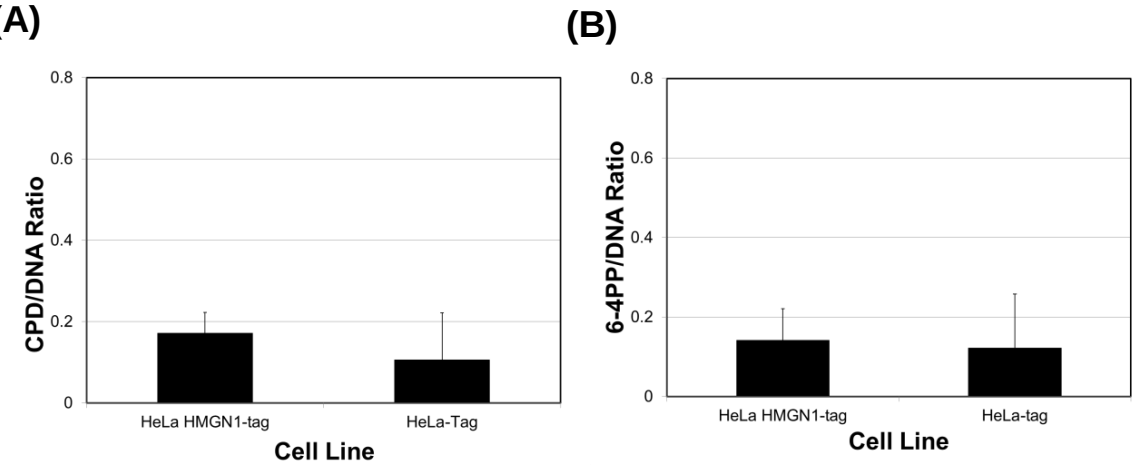

Figure 13: Photoproduct/DNA Ratio in HeLa HMGN1-tag and HeLa-tag Cells Immediately After UV Irradiation (0 hr)
The averages (±SE) of the CPD/DNA ratio (A) and 6-4PP/DNA ratio (B) at time 0 following UV irradiation of three independent repetitions of the experiment described. A nonparametric Mann Whitney U test showed that the HeLa HMGN1-tag cells were not significantly different from the HeLa-tag cells.

Effects of UV Irradiation on Global Acetylation Levels in Both HeLa-tag and HeLa HMGN1-tag Cells

Previous works have shown that the acetylation of core histones is involved in DNA repair (Birger et al., 2003; Sawan and Herceg, 2010; Yu et al., 2012). Research has also shown that HMGNs have the ability to modulate core histone post-translational modifications (Lim et al., 2005; Pogna et al., 2010; Postnikov et al., 2006). Reports have also shown that following UV induced DNA damage,

increased histone H3 acetylation at lysine 9 and 14 correlated with changes in chromatin structure, and these alterations were associated with efficient global genome nucleotide excision repair in yeast (Yu et al., 2011). Kinetics of core histone acetylation following UV irradiation of vertebrates was explored in DT40 chicken lymphoblast cells and a global wave of deacetylation was observed followed by a return to the original steady state levels of acetylation after 48-72 hours in histones H3K9, H3K14, and H4K5. However, core histone acetylation kinetics were not thoroughly explored in human cells (Subramanian, 2009). Therefore, we wanted to investigate the kinetics of core histone acetylation following UV irradiation specifically in human HeLa cells and what role the overexpression of HMGN1 plays in the acetylation of the chromatin and DNA repair.

To this end, the acetylation levels of core histones after UV irradiation in both the HeLa HMGN1-tag cells and HeLa-tag cells was explored. Cells were irradiated with UVC at 30 J/m^2 and acetylation levels of various lysines on both histone 3 and histone 4 were measured at various time points ranging from 30 minutes post UV irradiation to 72 hours post UV irradiation. To measure the acetylation levels, Western blot analysis was employed using antibodies against three post-translational modifications on histones: H3K9ac, H3K14ac, and H4K5ac (Figures 14, 15, 16, and 17).

Results from these assays are as follows: HeLa HMGN1-tag cells had a significantly higher basal level of acetylation of histone 3 lysine 9, and histone 3 lysine 14 as compared to HeLa-tag cells at time 0 hour. Although not significant, higher basal level of acetylation of histone 4 lysine 5 as compared to HeLa-tag cells was also seen. Four to 10 hours following UV irradiation all cell lines reached a trough of acetylation at each lysine site with pre UV steady state levels of acetylation being reestablished 24 to 72 hours after UV irradiation. On histone 3 lysine 9, the HeLa HMGN1-tag cells demonstrated 550% basal global acetylation, histone 3 lysine 14 displayed 170% higher basal acetylation levels, and histone 4 lysine 5 displayed 155% basal acetylation as compared to HeLa-tag cells (Figures 14, 15, and 16). These results suggest that HMGN1 plays a role in regulating post-translational modifications of histones before UV irradiation.

The robust decrease in core histone acetylation levels after UVC irradiation suggests that HMGN1 does play a role not only in acetylation but perhaps also in deacetylation of chromatin following UV damage. To confirm this theory experiments were performed to test whether HMGN1 is associated with specific histone acetyltransferases (HATs) or histone deacetyltransferases (HDACs) before and after UV irradiation.

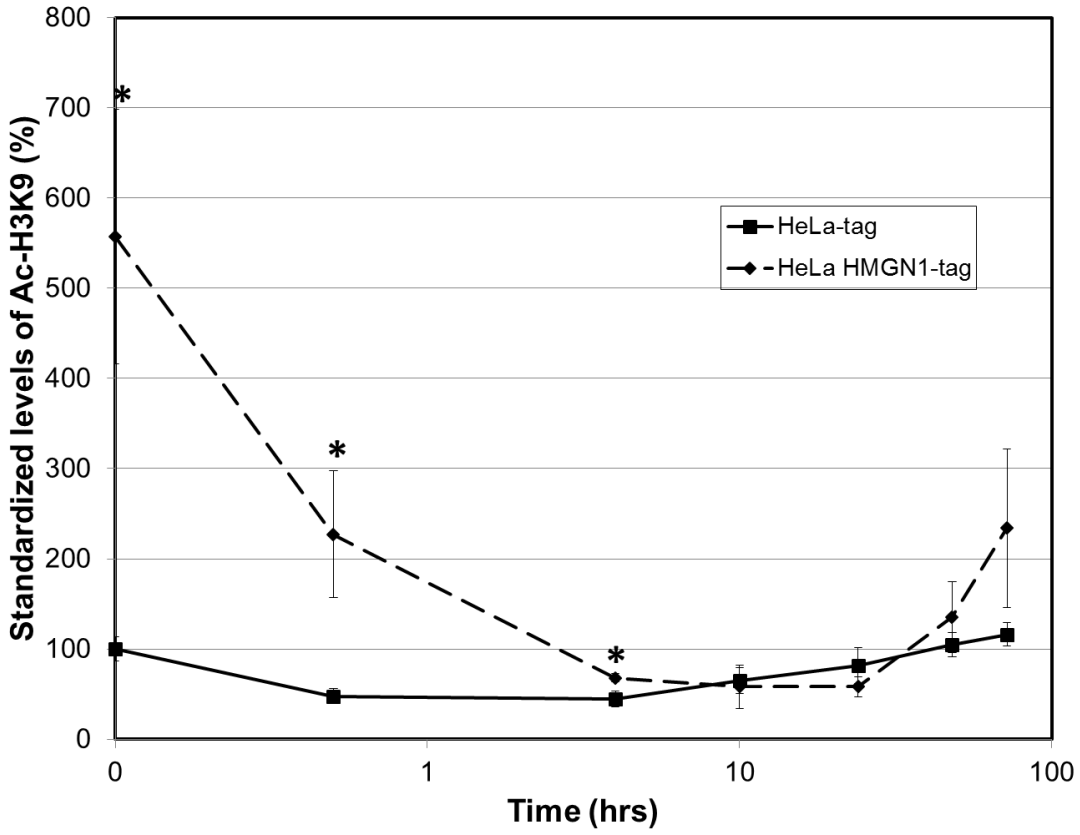

Figure 14: Acetylation Kinetics of H3K9 Post UV Irradiation
The cells were irradiated at 30 J/m^2 and lysed at various time intervals after UV irradiation and Western blot analysis against specific anti-H3K9ac antibody was carried out. Each data point represents the mean of three independent repetitions (± SE). The level of acetylation was measured by spot densitometry and standardized against level of the respective histone.
Note: Significant difference acetylation betweem HeLa-tag and HeLa HMGN1-tag is indicated by * as determined by Kruskal-Wallis test, ($p \leq 0.05$).

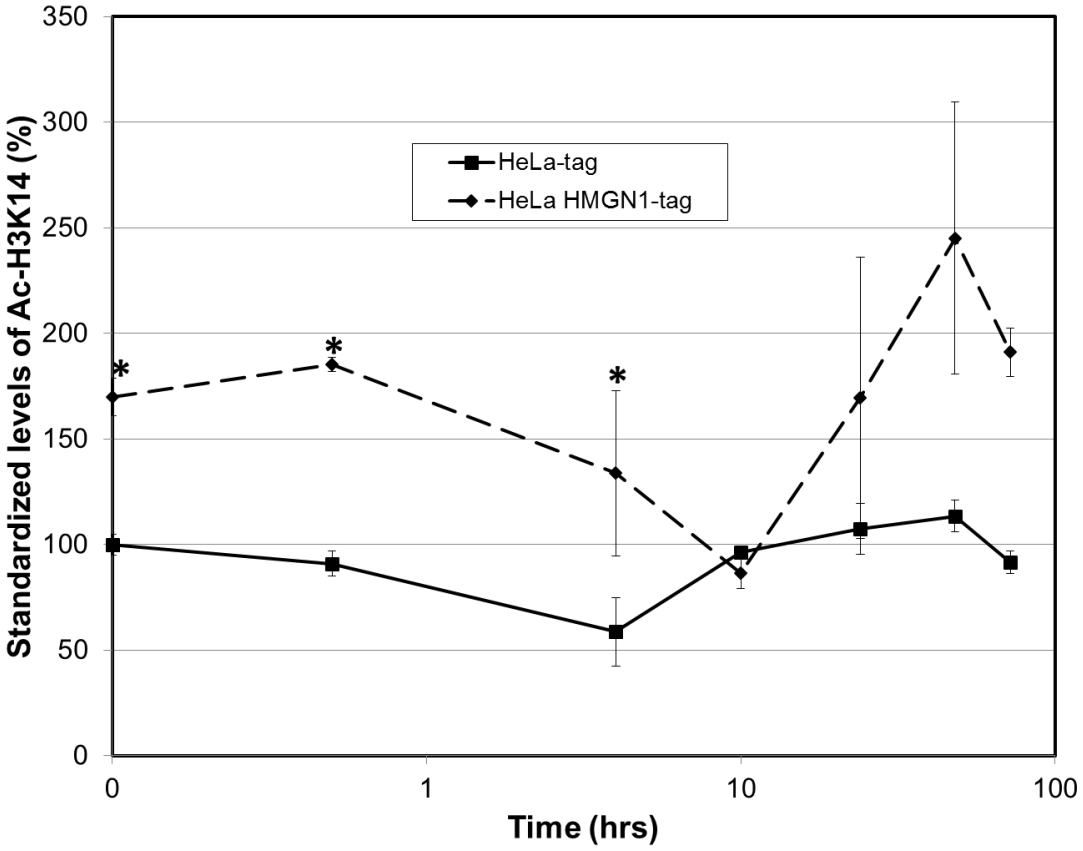

Figure 15: Acetylation Kinetics of H3K14 Post UV Irradiation

The cells were irradiated at 30 J/m^2 and lysed at various time intervals after UV irradiation and Western blot analysis against specific anti-H3K14ac antibody was carried out. Each data point represents the mean of three independent repetitions (± SE). The level of acetylation was measured by spot densitometry and standardized against level of the respective histone.

Note: Significant difference acetylation betweem HeLa-tag and HeLa HMGN1-tag is indicated by * as determined by Kruskal-Wallis test, ($p \leq 0.05$).

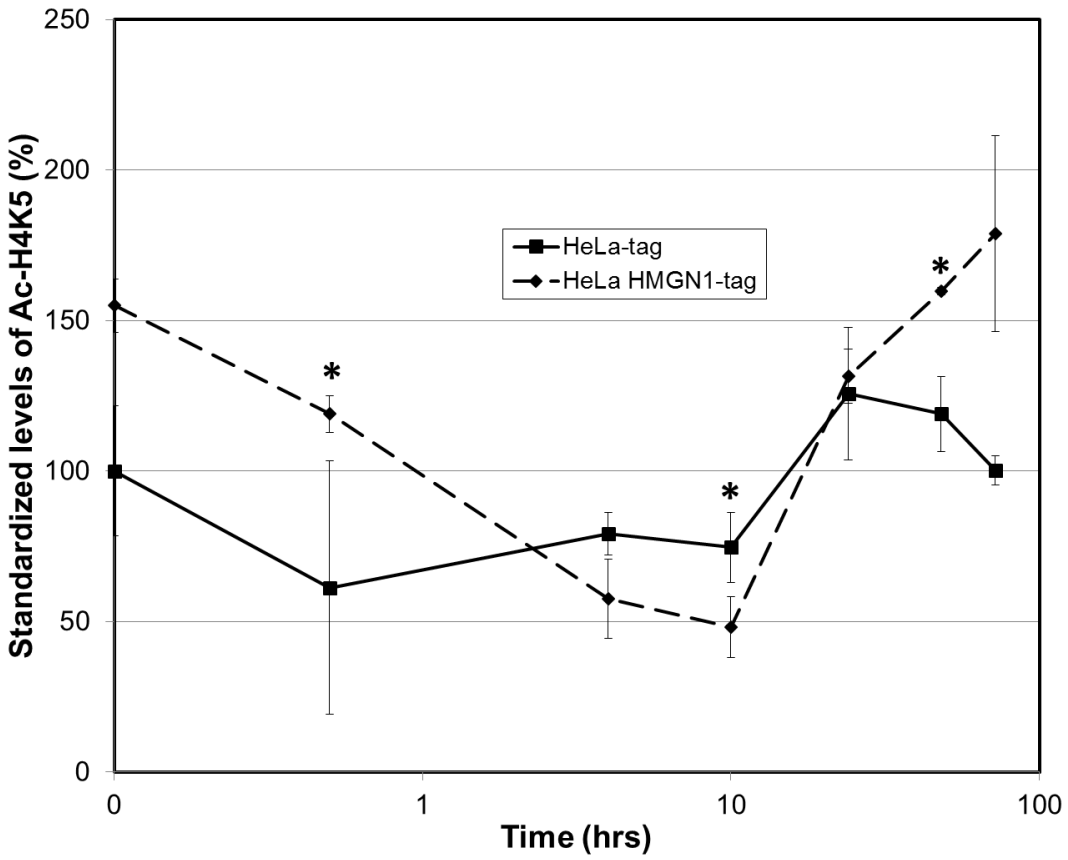

Figure 16: Acetylation Kinetics of H4K5 Post UV Irradiation
The cells were irradiated at 30 J/m^2 and lysed at various time intervals after UV irradiation and Western blot analysis against specific anti-H4K5ac antibody was carried out. Each data point represents the mean of three independent repetitions (± SE). The level of acetylation were measured by spot densitometry and standardized against level of the respective histone.
Note: Significant difference acetylation betweem HeLa-tag and HeLa HMGN1-tag is indicated by * as determined by Kruskal-Wallis test, ($p \leq 0.05$).

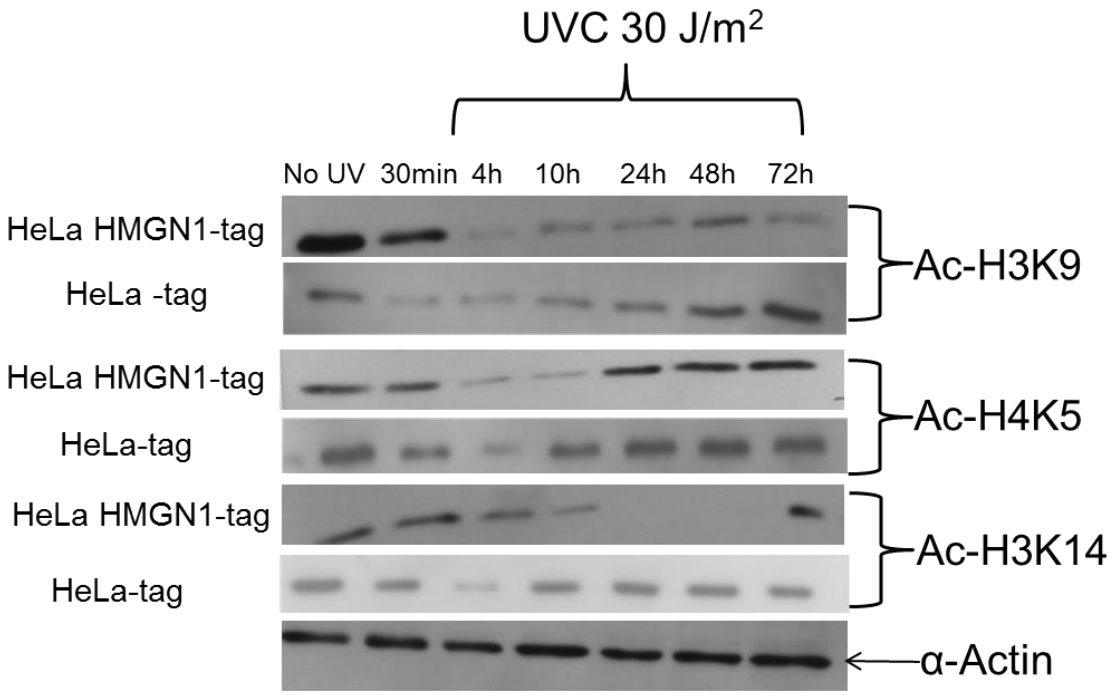

Figure 17: UV Irradiation Induces a Global Wave of Deacetylation of Core Histones in Both HeLa-tag and HeLa HMGN1-tag Cells

The top six rows represent Western blots displaying levels of three different acetyl lysines in histones H3 and H4 in both HeLa-tag and HeLa HMGN1-tag cells (as indicated). The bottom panel represents a Western blot against α-Actin, demonstrating equal loading of proteins. The cells were irradiated with UVC at 30 J/m^2 and extracted at various time intervals post UV irradiation. The proteins were resolved on 15% SDS-PAGE and subjected to Western blot using antibodies against: H3K9ac, H4K5ac, and H3K14ac. Each experiment was repeated three independent times and the graphical representative of the averages are show in Figures 14, 15, and 16.

HMGN1 is Associated with P300 and HDAC2

As mentioned, the results from human and chicken cells suggested that HMGN1 plays a role not only in acetylation but perhaps also in deacetylation of chromatin following UV damage (Lim et al., 2005). Therefore, whether HMGN1 interacts with HDACs and/or HATs was investigated. Human HDAC1 and HDAC2 have been shown to play a role in DNA-damage response following induction of double stranded breaks by ionizing radiation (Miller et al., 2010). Therefore, we wanted to determine whether HDAC1 and HDAC2 may be involved in NER and associated with HMGN1 before and after UV irradiation. Using HeLa HMGN1-tag cells immunoprecipitation assays were carried out using antibodies against either HDAC1 and HMGN1 or HDAC2 and HMGN1. Western blots using the reciprocal antibodies were performed to test for a possible association. It was determined that HMGN1 is associated with HDAC2 in non UV irradiated cells and *in vitro* (Figure 18 and Figure 19).

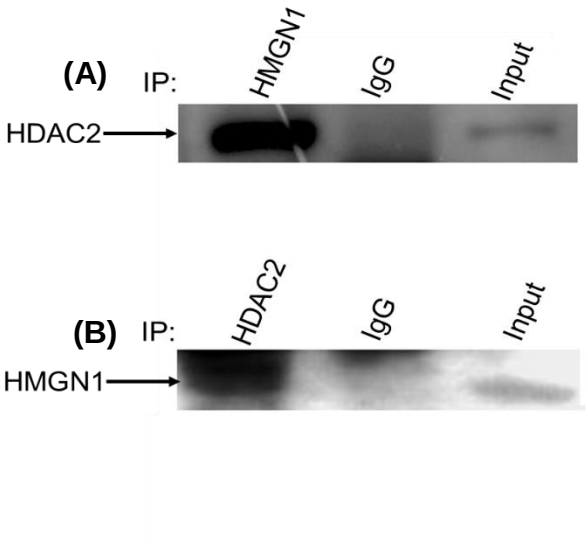

Figure 18: HMGN1 and HDAC2 are Associated Together in HeLa cells Immunoprecipitation showed an association between HMGN1 and HDAC2 in non-irradiated HeLa cells. (A) Immunoprecipitation with 10 µg of rabbit anti-HMGN1 antibody detected HDAC2 protein using goat anti-HDAC2 antibody in a Western blot (10% SDS-PAGE). (B) Immunoprecipitation with 4 µg of goat anti-HDAC2 detects HMGN1 protein by Western blot with rabbit anti-HMGN1 antibody (15% SDS-PAGE).

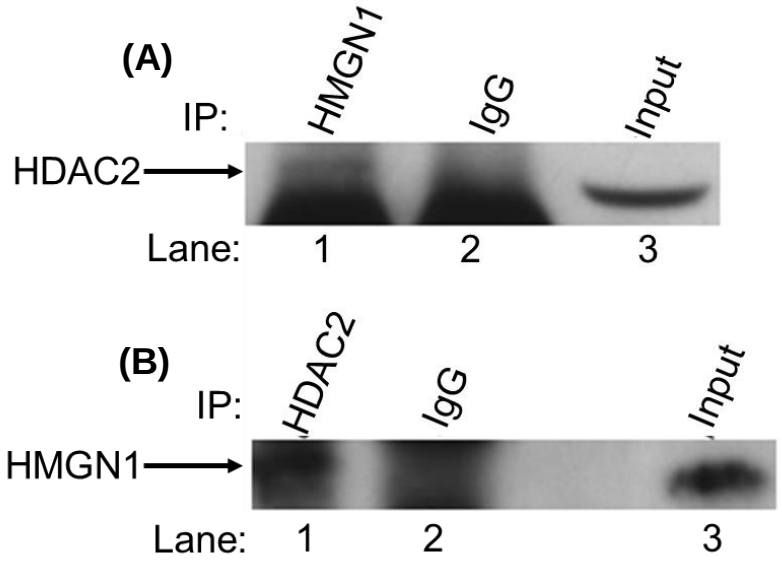

Figure 19: HMGN1 and HDAC2 Show an Association Following a Pull-down Assay
Pull-down assay showed an association between HMGN1 and HDAC2. A) Lane 1: 3.5 µg of recombinant HDAC2, 1.0 µg of recombinant HMGN1, and 9.0 µg of rabbit α-HMGN1 antibody. Lane 2: 3.5 µg of recombinant HDAC2, 1.0 µg of recombinant HMGN1, and 9.0 µg of rabbit non immune IgG antibody. Lane 3: recombinant HMGN1 (positive control). The proteins were resolved on 10% SDS-PAGE and subjected to a Western blot against anti-HDAC2 antibody. (B) Lane 1: 3.5 µg of recombinant HDAC2, 1.0 µg of recombinant HMGN1, and 3.0 µg of goat α-HDAC2 antibody. Lane 2: 3.5 µg of recombinant HDAC2, 1.0 µg of recombinant HMGN1, and 3.0 µg of goat non immune IgG antibody. Lane 3: recombinant HMGN1 (positive control). The proteins were resolved on 15% SDS-PAGE and subjected to a Western blot against rabbit α-HMGN1 antibody.

A similar immunoprecipitation was performed with HDAC1 and HMGN1 and an association was not seen prior to UV irradiation (Figure 20).

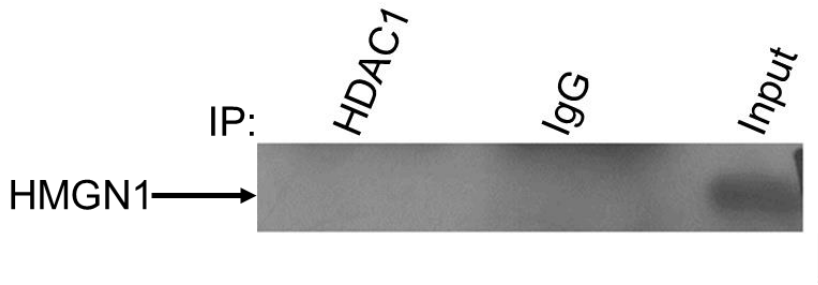

Figure 20: HMGN1 and HDAC1 are not Associated with Each Other in HeLa Cells
Immunoprecipitation with extracts from non-irradiated HeLa-tag cells showed no association between HMGN1 and HDAC1. Immunoprecipitation with 2 µg of goat anti-HDAC1 antibody did not detect HMGN1 protein using rabbit anti-HMGN1 antibody and a Western blot (15% SDS-PAGE).

Next, we attempted to determine the kinetics of HMGN1 and HDAC2 association following UV irradiation. Cells were UVC irradiated with 30 J/m^2 and lysed at 0, 1, 4, and 10 hours after UV irradiation and co-immunoprecipitation with antibodies against HMGN1 and HDAC2 was performed followed by Western blot with the reciprocal antibody (anti-HDAC2 and anti-HMGN1, respectively). The results coincided with the acetylation kinetics studies in that an association of HMGN1 with HDAC2 was observed at 1-10 hours following UV irradiation, which were the same time points when deacetylation started and reached it maximum peak (Figure 21). However, the levels of the HMGN1-HDAC2 complex were

similar between all time points and the pre-UV irradiation lysate, indicating that there are additional factors controlling core histone deacetylation.

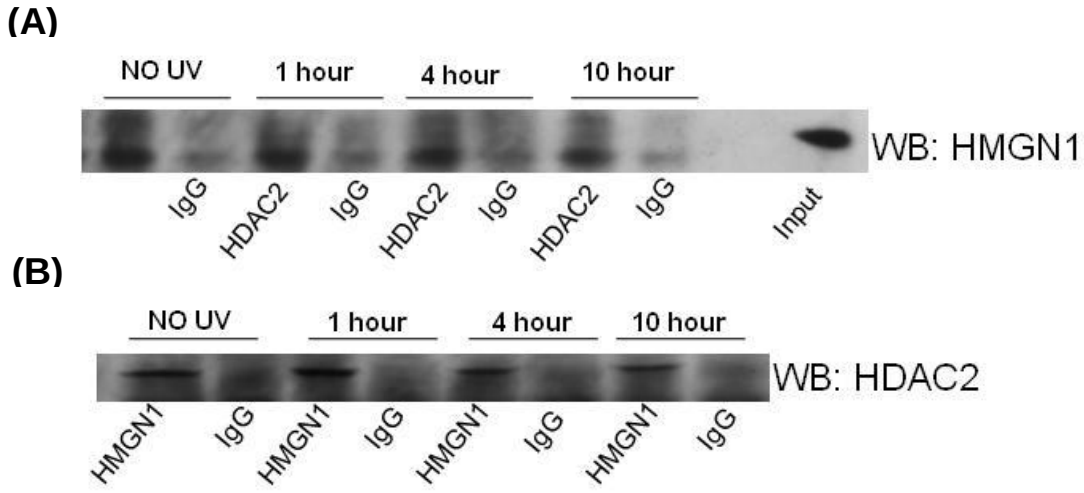

Figure 21: Association Between HMGN1 and HDAC2 Following UV Irradiation
Immunoprecipitation with 4 µg of goat anti- HDAC2 antibody detected HMGN1 protein with rabbit anti-HMGN1 antibody, used for Western blotting on a 15% SDS-PAGE at time 0, 1 hr, 4hr, and 10hr following UV irradiation. (B) Immunoprecipitation with 10 µg of anti-HMGN1 antibody detected HDAC2 protein with goat anti-HDAC2 antibody used for Western blotting on a 10% SDS-PAGE at time 0, 1 hr, 4hr, and 10hr following UV irradiation.

The HAT p300 was shown previously to acetylate HMGN1 (Bergel et al., 2000; Lim et al., 2005) and it was also found to be associated with newly synthesized DNA at UV induced damage sites (Hasan et al., 2001). Yet, an association between HMGN1 and HATs (including p300) was shown only in preliminary co-immunoprecipitation (co-IP) studies (Subramanian, 2009). Knowing that previous studies have shown that p300 (Fousteri et al., 2006; Tillhon et al., 2012) is involved in NER, test were performed to determine whether HMGN1 is associated with p300. To corroborate the association between p300 and HMGN1 a pull-down assay was performed using recombinant p300 and recombinant HMGN1 and p300 antibody. Coomassie staining was performed to detect the possible association of the two proteins. The results demonstrated that HMGN1 is associated with p300 *in vitro* (Figure 22).

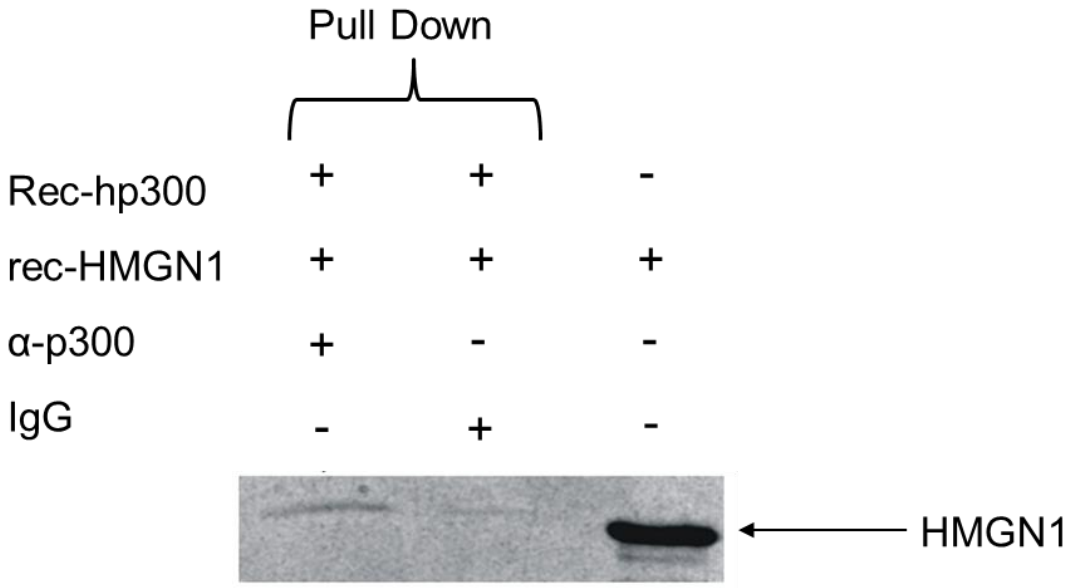

Figure 22: P300 and HMGN1 are Associated Together *In Vitro*
Pull down assay to determine p300 and HMGN1 association. Lane 1: 0.4 µg of recombinant human p300, 0.4 µg of recombinant HMGN1, and 1.0 µg of mouse α-p300 antibody. Lane 2: 0.4 µg of recombinant p300, 0.4 µg of recombinant HMGN1, and 1.0 µg of mouse non-immune IgG antibody. Lane 3: recombinant HMGN1 (control). The proteins were resolved on 15% SDS-PAGE and stained with Coomassie blue.

It has now been established that HMGN1 plays a role in modulating the global level of core histone acetylation and deacetylation before and after UV irradiation. The next experiment was aimed at determining the possible involvement of HMGN1 on DNA-damage repair sites.

Localization of HMGN1 During Early and Late Stages of NER

We have shown that HMGN1 is involved in DNA repair following UV induced damage, and that this involvement may be through HMGN1's association with HDAC2 and p300. To further confirm these results we used local UV irradiation and Immunofluorescence microscopy to determine the possible localization of HMGN1 during early and late stages of NER. Local UV irradiation is a method that allows visualization of DNA photoproducts and repair factors in a specific area within the nucleus. The UV irradiation of the cells was done at 100 J/m^2 through an isopore polycarbonate membrane filter (3 μm in size) which generated damage in spots. Cells were then treated with antibodies against HMGN1 and known NER repair proteins, Xeroderma pigmentosum complementation group C (XPC) and proliferating cell nuclear antigen (PCNA). XPC was used as the marker protein to determine the localization of HMGN1 at early stages of NER, and PCNA was used to determine the localization of HMGN1 at late stages of NER. Local UV irradiation showed that 5 minutes and 1 hour following UV irradiation, HMGN1 was partially colocalized with areas of UV damage. In comparison, local UV irradiation showed that 24 hours following UV irradiation HMGN1 was highly colocalized with areas of UV damage (Figures 23, 24, and 25).

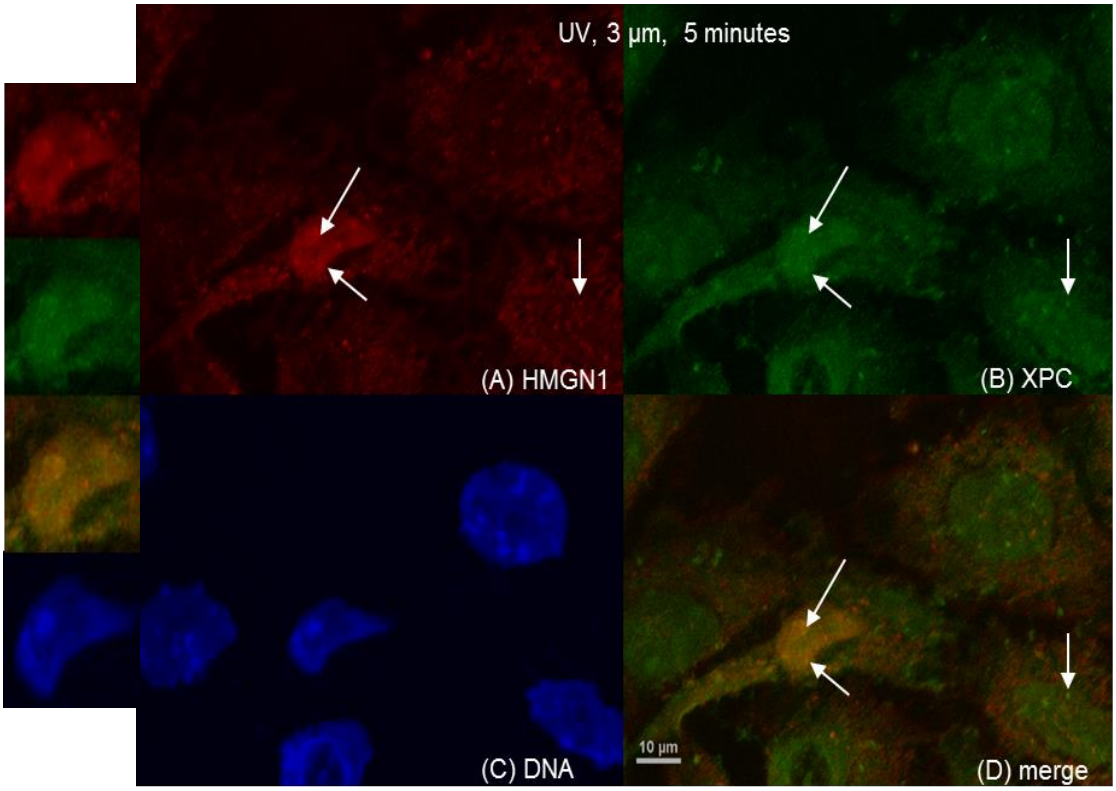

Figure 23: HMGN1 is Loosely Associated with Early Damaged Sites on the DNA 5 Minutes After UV Irradiation

Effect of local UV irradiation on the distribution of XPC and HMGN1 5 minutes after UVC irradiation. HeLa cells were locally UV irradiated with 100 J/m^2, using filters with 3 µm pores. Following irradiation, cells were incubated for 5 minutes and then immunostained with (A) anti-HMGN1 antibody, (B) anti-XPC antibody, and (C) Hoechst (DNA) staining followed by secondary fluorescently tagged antibodies directed against the primary antibodies. (D) merged image of HMGN1 and XPC.

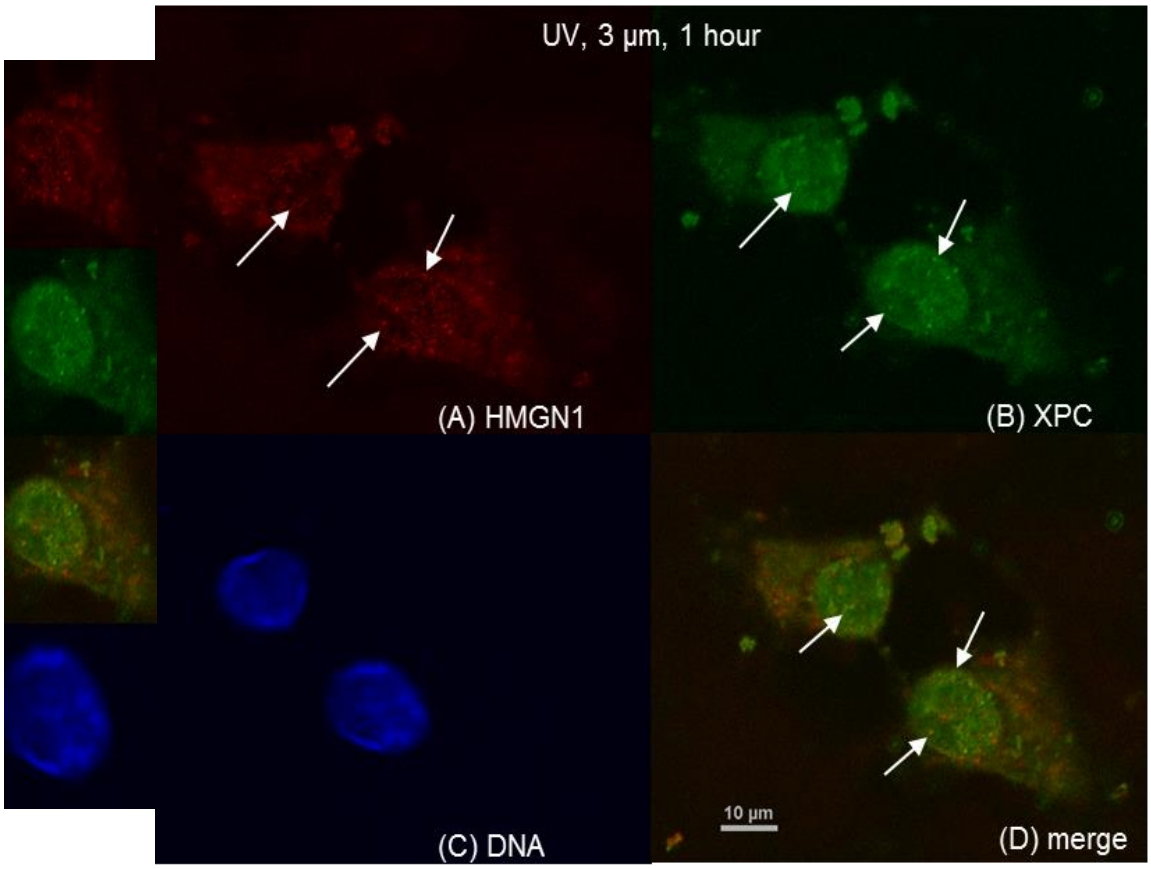

Figure 24: HMGN1 is Loosely Associated with Early Damaged Sites on the DNA 1 Hour After UV Irradiation

Effect of local UV irradiation on the distribution of XPC and HMGN1 1 hour after UVC irradiation. HeLa cells were locally UV irradiated with 100 J/m^2, using filters with 3 µm pores. Following irradiation, cells were incubated for 1 hour and then immunostained with (A) anti-HMGN1 antibody, (B) anti-XPC antibody, and (C) Hoechst (DNA) staining followed by secondary fluorescently tagged antibodies directed against the primary antibodies. (D) merged image of HMGN1 and XPC.

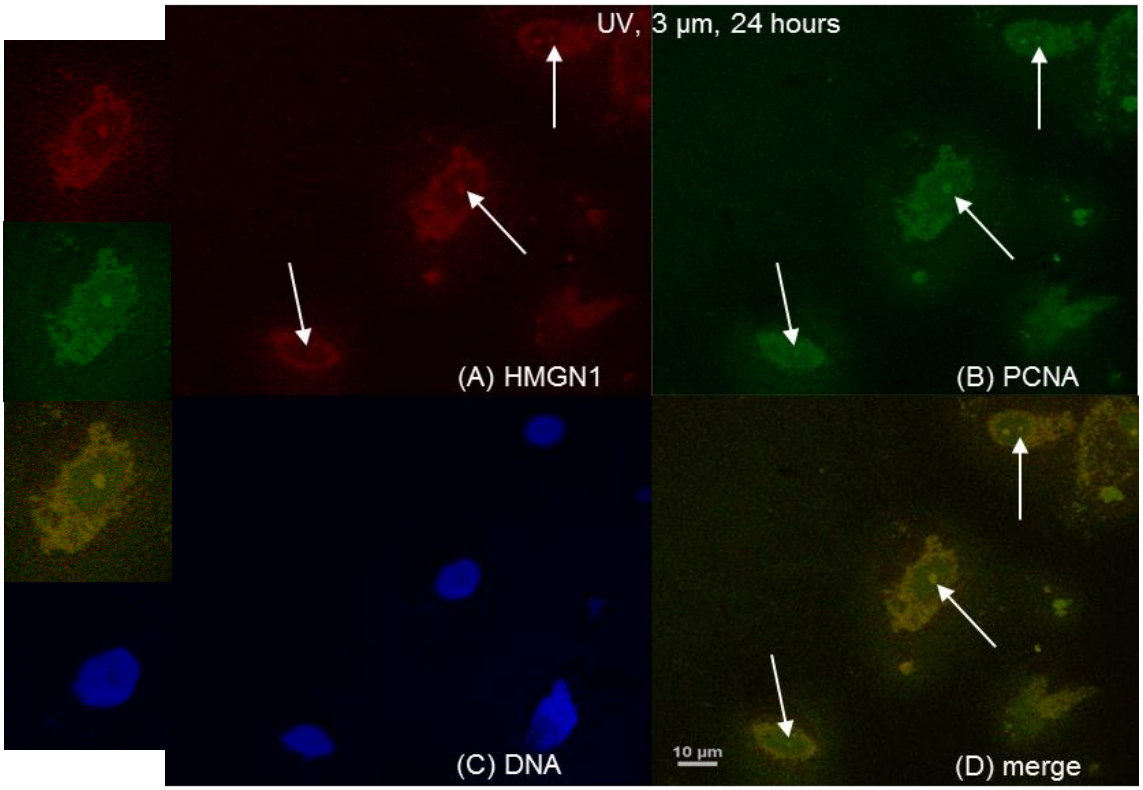

Figure 25: HMGN1 is Closely Associated with Late Damaged Sites on the DNA 24 Hours After UV Irradiation.
Effect of local UV irradiation on the distribution of PCNA and HMGN1 24 hours after UVC irradiation. HeLa cells were locally UV irradiated with 100 J/m^2, using filters with 3 µm pores. Following irradiation, cells were incubated for 24 hours and then immunostained with (A) anti-HMGN1 antibody, (B) anti-PCNA antibody, and (C) Hoechst (DNA) staining followed by secondary fluorescently tagged antibodies directed against the primary antibodies. (D) merged image of HMGN1 and PCNA.

Subcloning of Recombinant HMGN1

We have shown that overexpression of the HMGN1 protein in HeLa cells led to an enhanced cell survival and increased DNA repair rate. Using this information we eventually would like to test whether the topical application of HMGN1 protein to mice skin could lead to an enhanced cell survival and DNA repair rate. The HMGN1 protein we plan to purify was a gift from the lab of Dr. Bustin and was sent fused with the green fluorescent protein (GFP) protein. The first step in obtaining recombinant HMGN1 was to perform a PCR that produced the HMGN1 fragment without the GFP tag using primers that contained the EcoRI and BamHI restriction enzyme sites. Once the isolation of HMGN1 gene from GFP was confirmed by an agarose gel, restriction digests of both HMGN1 and a pMAL vector (the vector the HMGN1 gene was inserted into) were performed using EcoRI and BamHI, both of which are located on the vector and HMGN1 (Figure 26 and Figure 27).

(A)

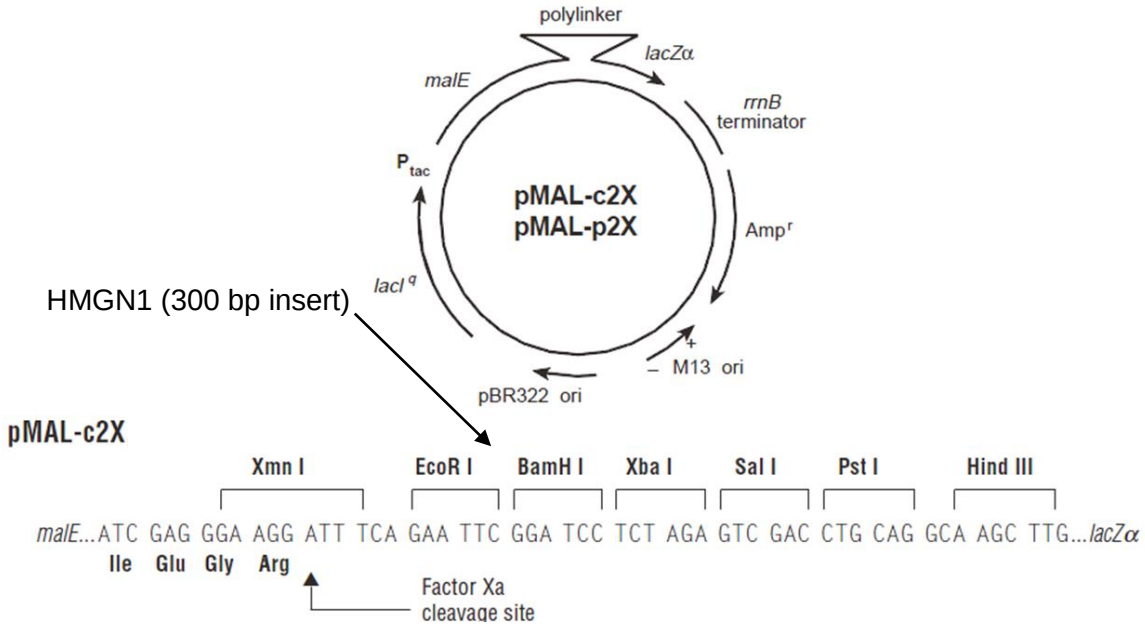

(B)

HMGN1:

Catgcccaagaggaaggtcagctccaccgaaggcgccgccaaggaagagcccaagaggagatcggcgc
ggttgtacagctaaacctcctgcaaagtgaaaaaggcagcagcgaaggataaatcttcagacaaaaaagtgc
aaacaaaagggaaaaggggagcaaagggaaaacaggccgaagtggctaaccaagaaactactgcgga
aaacggggaaacgaagactgaggagagtccagcctctgatgaagcaggagagaaagaagccaagtctga
ttaag

Forward primer:

tgaattcatgcccaagaggaaggtcagctc

Reverse primer:

gggatccttaatcagacttggcttctttct

Figure 26: PMAL Plasmid and DNA Sequence of HMGN1 with Primers
(A) pMAL plasmid including site of insertion for HMGN1. Plasmid taken from: https://www.neb.com/products/e8200-pmal-protein-fusion-and-purification-system#tabselect0 (B) DNA sequence of HMGN1, forward primer and reverse primer.

This restriction digest and the HMGN1 PCR product were confirmed using a 1.5% agarose gel for HMGN1 and a 0.7% agarose gel for the pMAL vector (Figure 27).

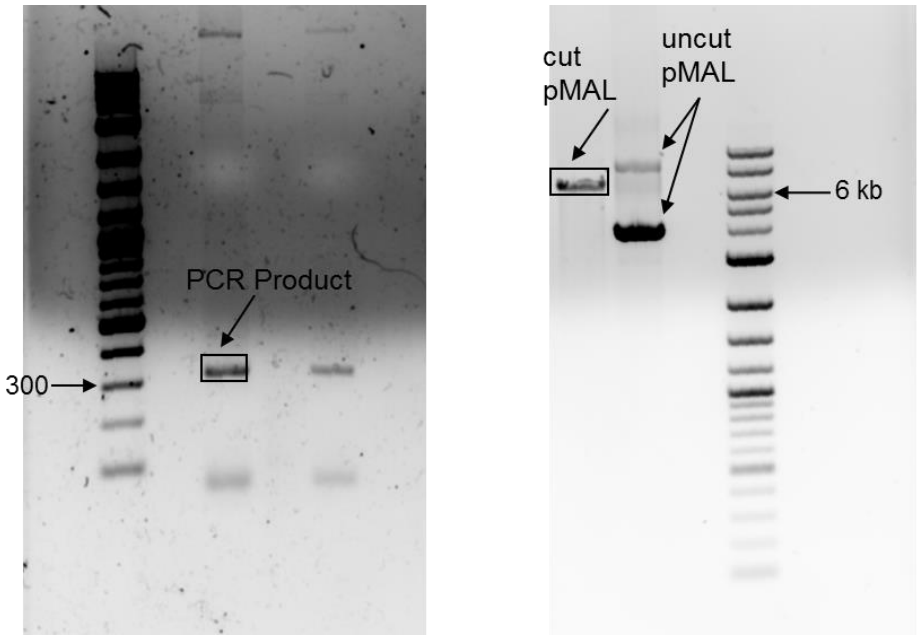

Figure 27: Products of the Restriction Digest of Both PMAL Vector® and HMGN1 PCR Product.
Restrictions digest of both pMAL vector and HMGN1 insert. **(A)** Restriction digest using restriction enzymes EcoRI and BamHI was performed on an amplified EcoRI-HMGN1-BamHI PCR product. Restriction digest was confirmed by resolving samples on 1.5% agarose gel. HMGN1 insert is seen as expected around 300 base pairs. **(B)** Restriction digest using restriction enzymes EcoRI and BamHI was performed on the pMAL vector. Restriction digest was confirmed by resolving samples on 0.7% agarose gel. Cut pMAL vector ran at ~6.6 kb, the expected size of the vector (see Materials & Methods).

Once confirmed, using a NEB quick ligation kit, the purified HMGN1 gene, and pMAL™ vector were ligated. We can assume the ligation of HMGN1 to the pMAL vector only occurred in the correct orientation because we used two restriction enzymes (EcoRI and BamHI) to generate sticky ends. The pMAL™ vector is used to assist in purifying proteins. This vector was specifically chosen because it includes the maltose-binding protein gene. This vector is designed so that the protein of interest (HMGN1) is inserted downstream from the *malE* gene which encodes the maltose-binding protein. This process results in expression of a MBP-HMGN1 fusion protein and also allows for large amounts of the protein of interest to be expressed and purified in a one step process (Riggs, 2001). Using DH5α cells a transformation was performed following ligation and the culture was plated and screened for “positive” colonies, some of which were expected to contain the subcloned HMGN1 gene. DNA was extracted from all clones that screened positive, and this DNA was subjected to PCR using the previous primers for HMGN1 PCR (Figure 26). These samples were then run on an agarose gel and it was confirmed that 3 out of 9 subclones contained the HMGN1 gene fused into the pMAL vector (Figure 28).

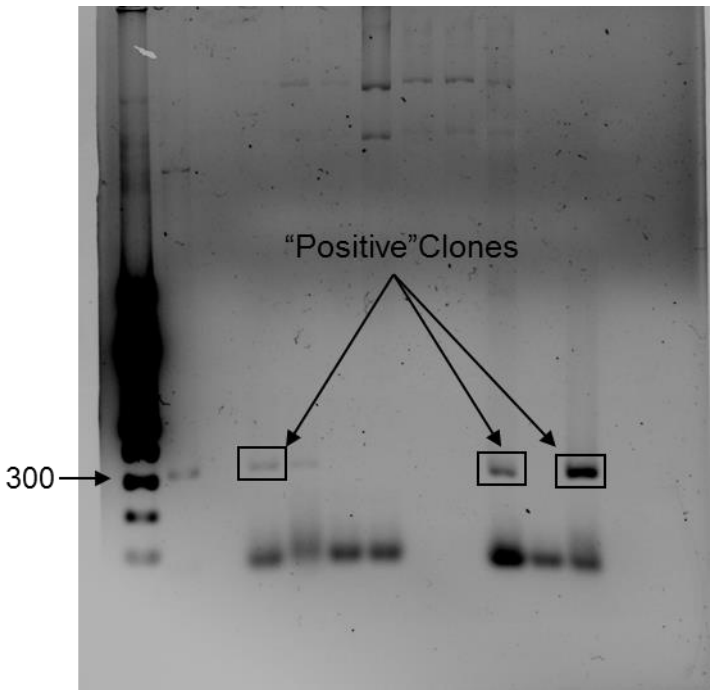

Figure 28: Confirmation of the Ligation of HMGN1 Insert into PMAL Vector.
Competent DH5α cells were transformed with the pMAL vector containing the HMGN1 insert. This culture was plated on LB+amp+X-Gal+IPTG plates and screened for "positive" colonies. These "positive" colonies (colonies that could potentially contain the plasmid with the ligated HMGN1 gene) should show up white. DNA from these colonies was extracted and subjected to PCR using primers for the HMGN1 gene. A 1.5% agarose gel was run to confirm that the subclones contained the gene of interest.

Both the DNA and clones plated from these samples were immediately frozen for later use. In the future, the lab would like to take this subcloned HMGN1 and purify recombinant HMGN1 using maltose columns. This recombinant HMGN1 protein will then be inserted into a topical agent such as liposomes (with help from outside sources) and applied to mice skin before and after UV irradiation. Following application, several tests will be performed to determine the effect of overexpression of HMGN1 protein on mice histology and DNA repair levels.

CHAPTER IV

DISCUSSION

HMGN1 Involvement in GG-NER Pathway in Human Cells

DNA repair requires a complex interaction between repair factors, chromatin remodelers, histone modifications, and other factors. These players work in concert to allow access to damaged sites for repair. It was previously reported that the HMGN1 protein plays a role in both the TC-NER subpathway in mice (Birger et al., 2003; Fousteri et al., 2006) and in the GG-NER subpathway in chicken (Subramanian et al., 2009) and is involved in modulating post-translational modifications of core histones (Postnikov et al., 2006; Ueda et al., 2006; Zhang and Wang, 2008). It is also known that DNA repair is associated with increased acetylation at damage sites (Guo et al., 2011; Smerdon et al., 1982; Vempati et al., 2010). The major goals in this work were to explore the possibility that overexpressing HMGN1 protein can protect cells from UV irradiation, improve the DNA repair rate, and to better understand the role of HMGN1 in DNA repair. The experiments conducted in this work also further investigated the hypothesis that HMGN1's role in DNA repair may be through its association with HATs and HDACs. The results obtained not only corroborated the role of HMGN1 in NER but extended them to human cells, and also helped to better understand HMGN1's specific involvement in DNA repair following UV

irradiation. The experiments demonstrated an association between the nucleosomal-binding protein HMGN1 activity in the NER pathway and the regulation of core histone acetylation and deacetylation. Previously, it was shown that the loss of HMGN1 in mouse embryonic fibroblasts (MEFs) reduced the rate of DNA repair (Birger et al., 2003) and that the loss of HMGN2 in chicken lymphoblastoid cells resulted in a reduction in the CPD removal rate and cell survival rate (Subramanian et al., 2009). Subramanian et al., also suggested that HMGN2 may facilitate accessibility of DNA repair machinery to DNA damage sites, specifically in the GGR subpathway. The results presented in this work supported the involvement of HMGN1 in DNA repair and broaden their scope to HMGNs role in GG-NER pathway of human cells, which to our knowledge had not been previously reported. Specifically, cells that had an increased level of HMGN1 protein were used and an increase in the cell survival rate was observed. Next, the hypothesis that the increase in cell survival rate was due to a growth advantage of the HeLa HMGN1-tag cells was tested. A growth curve study was performed and no significant differences were observed between the control HeLa-tag cells and the ovexpressing HeLa HMGN1-tag cells.

An alternative explanation for the enhanced cell survival rate of HMGN1 overepressor cells following UV damage was that these cells had an increased DNA repair rate. Employing Southwestern blot anaylsis, we indeed found that the overexpression of the HMGN1 protein correlated with increased removal rate of

both CPDs and 6-4PPs following UV irradiation. Therefore, the conclusion is that the hyposensitivy of the HeLa HMGN1-tag cells was perhaps because of a faster or enhanced DNA repair rate. In the future, with further experimentation, the HMGN1 protein could have significant clinical implications. It has been observed that HMGN1 overexpressing cells have an enhanced cell survival and DNA repair rate. Using a topical agent, an abundance of recombinant HMGN1 protein could be applied to the skin following exposure to UV light, possibly allowing for decreased DNA damage and enhanced repair of DNA damage. Consequently, the hypothesis that abundance of this protein could reduce the rate of skin cancers will be tested.

Increase of HMGN1 not HMGN2 Leads to Enhanced Cell Survival Rate

Although it appears that HMGN2 plays a role in DNA repair during GG-NER in chicken cells (Subramanian et al., 2009), we could not substantiate HMGN2's role in NER in human HeLa cells. The cell survival assay showed no significant difference between the control HeLa-tag cells to overexpressing HeLa HMGN2-tag cells. HMGN2 could still be important for DNA repair but the assay focused on the increase in protein levels rather than their depletion. If it is assumed that HMGN1 proteins levels are rate limiting, while HMGN2 levels are not, increasing the levels of HMGN1 may have the ability to significantly enhance the overall DNA repair process, while increased HMGN2 protein levels will not lead to enhanced DNA repair.

HMGNs Modulate Post-Translational Modifications Following UV Irradiation

There are various mechanisms in place to allow cells to recognize DNA damage and switch between the different repair pathways as needed (Peterson and Cote, 2004). One repair mechanism theory is that the binding of HMGN proteins to the nucleosome allow for the unfolding of the chromatin, which in turn allows access for repair machinery. Previous studies showed that when mutated forms of HMGN1 were expressed in HMGN1 -/- knockout mice cells, (these mutated HMGN1 were unable to bind to the nucleosomes or unfold chromatin) the cells remained hypersensitive to UV irradiation (Birger et al., 2003). Thus, binding to the nucleosomes enables HMGN1 to alter the chromatin structure both locally (at the damage site) and globally. This alteration of the chromatin structure by HMGN proteins is due in part to HMGNs ability to modulate the acetylation levels of core histones (Lim et al., 2004; Lim et al., 2005; Postnikov et al., 2006) and the acetylation of core histones is essential for DNA repair (Birger et al., 2003; Sawan and Herceg, 2010; Yu et al., 2012). It has also been shown that HMGN proteins regulate post translational modifications following stress response such as ionizing radiation (Kim et al., 2009). Based on this information, our experiments probed into the mechanism that leads to enhanced DNA repair and cell survival by testing the hypothesis that the enhanced cell survival and DNA repair rate of the HMGN1 overexpressing HeLa cells was partially due to the modulation of the core histone post-translational modifications, specifically acetylation and deacetylation. Lim et

al. showed that histone 3 acetylation on lysine 14 was reduced in HMGN1 -/- mouse embryonic fibroblasts (MEFs), but when these knockout cells were transfected with wild-type HMGN1 the basal acetylation levels were recovered (Lim et al., 2005). Our results that demonstrated increased H3K14 acetylation of HMGN1 in overexpressing HeLa cells are in accord with the report by Lim et al. in MEFs. Furthermore, our results showed that the overexpression of HMGN1 protein leads to increased basal acetylation levels in H3K9 and in H4K5 as well and that HMGN1 is associated with the HATs p300 and CBP both before and after UV irradiation (Subramanian, 2009). More specifically, Subramanian et al. observe an association between HMGN1 and CBP immediately (2 and 10 minutes) following UV irradiation and during the later stages of the NER pathway (24 hours) (Subramanian, 2009). This association between HMGN1, p300, and CBP is significant as previous findings showed that HMGN1 and p300 being independently involved in the TC-NER process (Fousteri et al., 2006) but not directly associated in one complex.

In addition to these findings, the experiments performed revealed that both the HeLa-tag and HeLa HMGN1-tag cell lines displayed a global wave of deacetylation that peaked between 4-10 hours following UV irradiation. To the best of our knowledge, this specific phenomenon has not been previously reported. While some reports demonstrated a deacetylation following UV irradiation (Battu et al., 2011; Fan and Luo, 2010), none of these reports demonstrated a time course

kinetics study. It is important to note that the basal levels of acetylation of H3K9, H3K14, and K4K5 in HeLa-HMGN1 tag cells was higher than HeLa-tag cells, yet the level of acetylation decreased much more robustly in the HeLa-HMGN1-tag cells in comparison to HeLa-tag cells. Both cell lines reached peak levels of deacetylation 4-10 hours post UV irradiation, and the cell lines returned to steady state levels of acetylation 24-48 hours after UV irradiation. We also observed that HMGN1 associated with HDAC2 at the same times as the deacetylation peaked. This suggests the association of HMGN1s with HDACs during the initial stages of the NER process. These results complement and do not contradict previous findings that indicated that the higher acetylation rate allows for the damaged chromatin sites to be more “open” following UV irradiation to allow easier access of repair machinery (Guo et al., 2011; Vempati et al., 2010). Combined, these results could also infer that deacetylation, globally, the presence of HMGNs, and local acetylation at the lesion sites are necessary for repair following UV irradiation.

HMGN1 Associates with HDAC2 Protein

To date, most information about HDACs and DNA repair shows the importance of HDAC inhibition, but not HDAC activation for better repair. The underlying theory is that the acetylation of core histones allows the unfolding of chromatin and therefore increases the access of the repair machinery to the DNA-damage site (Robert and Rassool, 2012). Miller et al., however, showed that the hypoacetylation of histone 3 was important in double strand break (DSB) repair

and that both HDAC1 and HDAC2 were involved in the DSB repair process (Miller et al., 2010). Also, while it is possible for some HATs and HDACs to bind nonspecifically to chromatin, data suggest that they specifically interact with various chromatin-associated binding factors and this association tethers the HATs and HDACs to chromatin (Bannister and Kouzarides, 2011; Narlikar et al., 2002). These results may suggest the possible involvement of HDACs in human HeLa cells GG-NER as well. Here it is shown that HDAC2 (but not HDAC1) was associated with HMGN1 both *in vivo* and *in vitro*, which may suggest that this association plays a role in the global wave of core histone deacetylation following UV irradiation. This wave of deacetylation appeared in both HeLa-tag and HeLa HMGN1-tag cells as well as in chicken DT40 cells and appeared to be involved in NER since the HDAC inhibitor TSA reduced the repair rate in both wild type DT40 cells as well as in HMGN1/2 knockout cells (Subramanian, 2009).

HMGN1 Localization with Spots of DNA Damage after UV Irradiation

The possible involvement of HMGNs in this wave of deacetylation as well as HMGNs involvement in UV-induced lesion removal are both events that happen early in the NER response. On the other hand, the involvement of HMGN1 at the late stages of NER was suggested by experiments using local UV irradiation followed by confocal microscopy analysis that demonstrated the colocalization of HMGN1 with PCNA, 24 hours after UV irradiation. Support for HMGN1's function in the post-incision complex assembly stages of TC-NER as well as its association

with Cockayne Syndrome A protein (CSA) was demonstrated previously (Fousteri et al., 2006). These results suggest that HMGN1 is involved in late stages of NER, perhaps at the stages of DNA-synthesis or post-synthesis chromatin remodeling. These results are also consistent with the lack of reacetylation of core histones in HMGN1/2 null chicken cells 24-72 hours after UV irradiation. This late involvement of HMGN1 in NER is in addition to its early involvement as could be visualized by the impaired repair of CPDs showing in HMGN1/2 null chicken cells (Subramanian et al., 2009) and the more efficient CPD and 6,4PP removal observed in HeLa HMGN1-tag cells.

Proposed Model: Role of HMGN1 in DNA Repair

Based on results obtained in this and previous works it is proposed that the coordinated associations of HMGN1 with HATs and HDACs following UV irradiation promote the compaction and decompaction of chromatin in DNA-lesion flanking areas and that ultimately leads to a more efficient repair of the damaged sites. Thus, it is suggested that HMGN1 modulates the DNA repair rate in a multi-step process. Prior to UV irradiation HMGN1 is associated with both p300 and HDAC2, helping to maintain the steady state levels of acetylation. Following UV damage, HMGN1 dissociates from its interaction with HATs at transcription sites (possibly by acetylation of HMGN1), and it associates preferentially with HDAC2 on the flanking regions of the damage site ensuring that they remain compacted. HMGN1's association with HDAC2 and binding to the lesion flanking regions

prevent further unwinding and excision of the damaged DNA strand, and allowing for a more focused, targeted, and efficient DNA repair, only at the unfolded chromatin at the damaged sites. In the second phase of the repair, the working hypothesis suggests that HMGN1 is involved in recruiting HATs and other factors which may participate in the re-establishment of the pre-UV irradiation epigenetic architecture at DNA lesion sites and possibly at the flanking regions as well (Figure 29).

HMGN proteins are known chromatin modifiers that play a role in transcription replication, and DNA repair (Birger et al., 2003; Morrison and Shen, 2005; Peterson and Cote, 2004; Subramanian et al., 2009; Ura and Hayes, 2002). These studies have established what appears to be a multi-functional role for the HMGN1 protein following UV irradiation of human cells. Along with previous studies, results done in this work suggest that not only does the HMGN1 protein play a role in DNA repair, but this role may be through a sequential recruitment of specific HDACs and HATs to and around the chromatin of the DNA-lesion sites (Subramanian, 2009). This in turn leads to dynamic epigenetic changes around and at the photo-lesions sites and thus modifying the chromatin structure to allow for a faster repair and post-excision chromatin recovery.

In the future, HMGN1 protein could have significant clinical implications. It has been observed that HMGN1 overexpressing cells have an enhanced cell survival and DNA repair rate. A topical agent (i.e., sunscreen) with recombinant

HMGN1 protein could be applied to the mice skin before and after exposure to UV light to examine the effect an abundance of the protein has on cells. If successful, this application could lead to decreased DNA damage and enhanced repair of DNA damage in skin cells and could prove beneficial to both healthy people overexposed to the sun and people with genetic disorders such as XP. Yarosh observed promising results delivering endonucleases via a liposome lotion to XP patients (Yarosh, 2004). A reduced rate of actin keratosis and skin cancer was observed following application of the lotion for 1 year. Based on these combined results, in theory, high levels of this protein could reduce the risk for skin cancers.

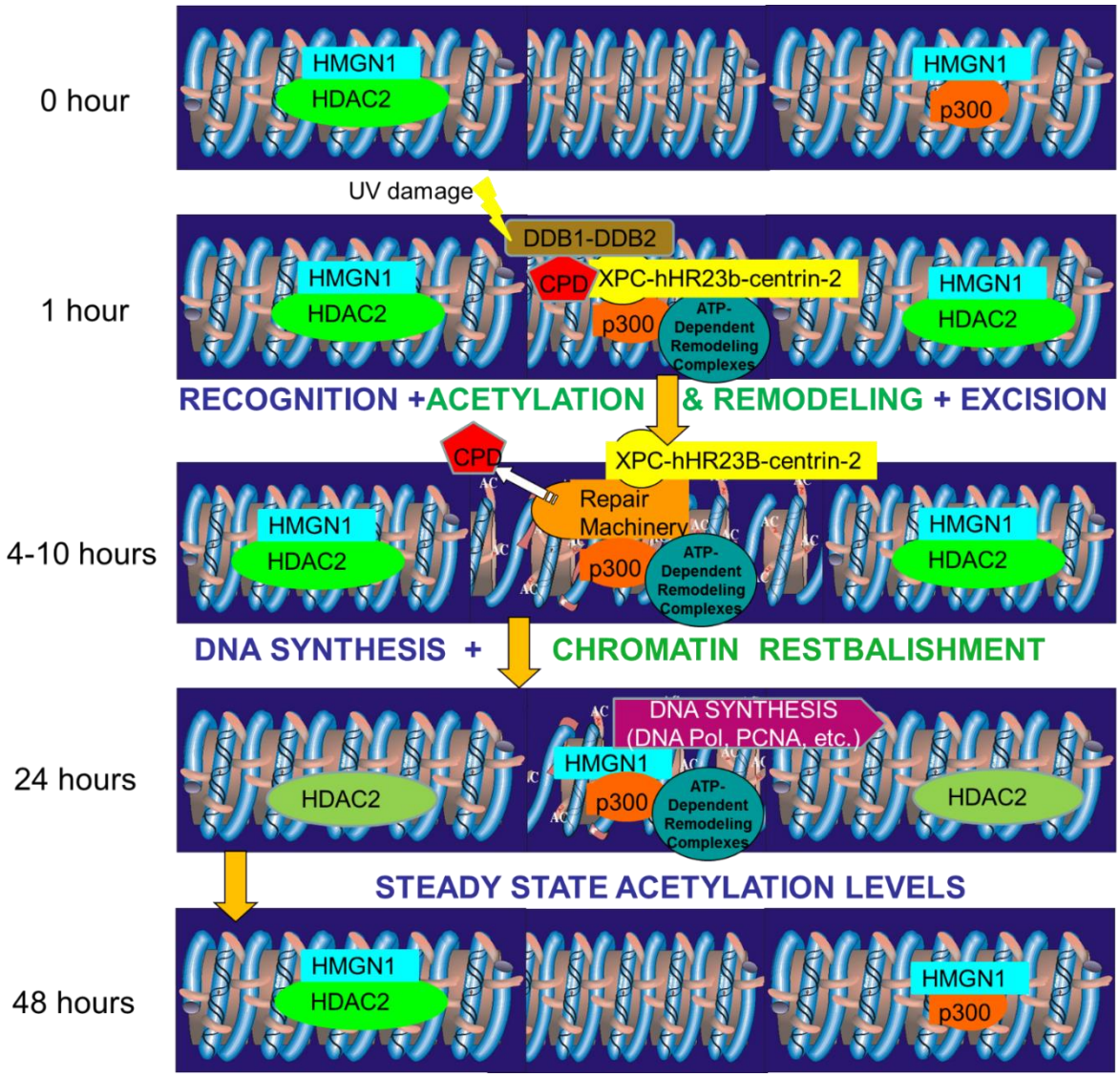

Figure 29: Proposed Model for the Role of HMGN1 in DNA Repair.
Proposed model for DNA repair following UV irradiation. This model demonstrates the possible roles of HMGN1 in the repair of DNA damage.

REFERENCES

Aboussekhra, A., and Thoma, F. (1999). TATA-binding protein promotes the selective formation of UV-induced (6-4)-photoproducts and modulates DNA repair in the TATA box. The EMBO Journal *18*, 433-443.

Adair, J.E., Kwon, Y., Dement, G.A., Smerdon, M.J., and Reeves, R. (2005). Inhibition of nucleotide excision repair by high mobility group protein HMGA1. The Journal of Biological Chemistry *280*, 32184-32192.

Adam, S., and Polo, S.E. (2012). Chromatin dynamics during nucleotide excision repair: histones on the move. International Journal of Molecular Sciences *13*, 11895-11911.

Aydin, O.Z., Vermeulen, W., and Lans, H. (2014). ISWI chromatin remodeling complexes in the DNA damage response. Cell Cycle *13*, 3016-3025.

Bannister, A.J., and Kouzarides, T. (2011). Regulation of chromatin by histone modifications. Cell Research *21*, 381-395.

Battu, A., Ray, A., and Wani, A.A. (2011). ASF1A and ATM regulate H3K56-mediated cell-cycle checkpoint recovery in response to UV irradiation. Nucleic Acids Research *39*, 7931-7945.

Belova, G.I., Postnikov, Y.V., Furusawa, T., Birger, Y., and Bustin, M. (2008). Chromosomal protein HMGN1 enhances the heat shock-induced remodeling of Hsp70 chromatin. The Journal of Biological Chemistry *283*, 8080-8088.

Bergel, M., Herrera, J.E., Thatcher, B.J., Prymakowska-Bosak, M., Vassilev, A., Nakatani, Y., Martin, B., and Bustin, M. (2000). Acetylation of novel sites in the nucleosomal binding domain of chromosomal protein HMG-14 by p300 alters its interaction with nucleosomes. The Journal of Biological Chemistry *275*, 11514-11520.

Bhakat, K.K., Hazra, T.K., and Mitra, S. (2004). Acetylation of the human DNA glycosylase NEIL2 and inhibition of its activity. Nucleic Acids Research *32*, 3033-3039.

Birger, Y., Catez, F., Furusawa, T., Lim, J.H., Prymakowska-Bosak, M., West, K.L., Postnikov, Y.V., Haines, D.C., and Bustin, M. (2005). Increased tumorigenicity and sensitivity to ionizing radiation upon loss of chromosomal protein HMGN1. Cancer Research *65*, 6711-6718.

Birger, Y., West, K.L., Postnikov, Y.V., Lim, J.H., Furusawa, T., Wagner, J.P., Laufer, C.S., Kraemer, K.H., and Bustin, M. (2003). Chromosomal protein HMGN1 enhances the rate of DNA repair in chromatin. The EMBO Journal *22*, 1665-1675.

Bustin, M., and Reeves, R. (1996). High-mobility-group chromosomal proteins: architectural components that facilitate chromatin function. Progress in Nucleic Acid Research and Molecular Biology *54*, 35-100.

Chang, L.C., Sheu, H.M., Huang, Y.S., Tsai, T.R., and Kuo, K.W. (1999). A novel function of emodin: enhancement of the nucleotide excision repair of UV- and cisplatin-induced DNA damage in human cells. Biochemical Pharmacology *58*, 49-57.

Choi, J.Y., Park, J.M., Yi, J.M., Leem, S.H., and Kang, T.H. (2015). Enhanced nucleotide excision repair capacity in lung cancer cells by preconditioning with DNA-damaging agents. Oncotarget *6*, 22575-22586.

Ehrenhofer-Murray, A.E. (2004). Chromatin dynamics at DNA replication, transcription and repair. European Journal of Biochemistry / FEBS *271*, 2335-2349.

Ellis, N.A. (1997). DNA helicases in inherited human disorders. Current Opinion in Genetics & Development *7*, 354-363.

Fan, W., and Luo, J. (2010). SIRT1 regulates UV-induced DNA repair through deacetylating XPA. Molecular Cell *39*, 247-258.

Fei, J., Kaczmarek, N., Luch, A., Glas, A., Carell, T., and Naegeli, H. (2011). Regulation of nucleotide excision repair by UV-DDB: prioritization of damage recognition to internucleosomal DNA. PLoS Biology *9*, e1001183.

Felsenfeld, G., and Groudine, M. (2003). Controlling the double helix. Nature *421*, 448-453.

Fernandez-Capetillo, O., and Nussenzweig, A. (2004). Linking histone deacetylation with the repair of DNA breaks. Proceedings of the National Academy of Sciences of the United States of America *101*, 1427-1428.

Fousteri, M., and Mullenders, L.H. (2008). Transcription-coupled nucleotide excision repair in mammalian cells: molecular mechanisms and biological effects. Cell Research *18*, 73-84.

Fousteri, M., Vermeulen, W., van Zeeland, A.A., and Mullenders, L.H. (2006). Cockayne syndrome A and B proteins differentially regulate recruitment of chromatin remodeling and repair factors to stalled RNA polymerase II in vivo. Molecular Cell *23*, 471-482.

Friedbergy E.C., W.G.C., Siede Wolfram, Wood Richard D., Schultz Roger A., and Ellenberger Tom (2006). DNA Repair and Mutagenesis, 2 edn (ASM Press).

Gaillard, P.H., Moggs, J.G., Roche, D.M., Quivy, J.P., Becker, P.B., Wood, R.D., and Almouzni, G. (1997). Initiation and bidirectional propagation of chromatin assembly from a target site for nucleotide excision repair. The EMBO Journal *16*, 6281-6289.

Gerlitz, G. (2010). HMGNs, DNA repair and cancer. Biochimica et Biophysica Acta *1799*, 80-85.

Gray, S.G., and Teh, B.T. (2001). Histone acetylation/deacetylation and cancer: an "open" and "shut" case? Current Molecular Medicine *1*, 401-429.

Green, C.M., and Almouzni, G. (2002). When repair meets chromatin. First in Series on Chromatin Dynamics. EMBO reports *3*, 28-33.

Grossman, S.R. (2001). p300/CBP/p53 interaction and regulation of the p53 response. European Journal of Biochemistry / FEBS *268*, 2773-2778.

Guo, R., Chen, J., Mitchell, D.L., and Johnson, D.G. (2011). GCN5 and E2F1 stimulate nucleotide excision repair by promoting H3K9 acetylation at sites of damage. Nucleic Acids Research *39*, 1390-1397.

Hara, R., Mo, J., and Sancar, A. (2000). DNA damage in the nucleosome core is refractory to repair by human excision nuclease. Molecular and Cellular Biology *20*, 9173-9181.

Hasan, S., Hassa, P.O., Imhof, R., and Hottiger, M.O. (2001). Transcription coactivator p300 binds PCNA and may have a role in DNA repair synthesis. Nature *410*, 387-391.

Kao, J., Rosenstein, B.S., Peters, S., Milano, M.T., and Kron, S.J. (2005). Cellular response to DNA damage. Annals of the New York Academy of Sciences *1066*, 243-258.

Kapoor, A., Agius, F., and Zhu, J.K. (2005). Preventing transcriptional gene silencing by active DNA demethylation. FEBS Letters *579*, 5889-5898.

Kim, Y.C., Gerlitz, G., Furusawa, T., Catez, F., Nussenzweig, A., Oh, K.S., Kraemer, K.H., Shiloh, Y., and Bustin, M. (2009). Activation of ATM depends on chromatin interactions occurring before induction of DNA damage. Nature Cell Biology *11*, 92-96.

Komori, H., Masui, R., Kuramitsu, S., Yokoyama, S., Shibata, T., Inoue, Y., and Miki, K. (2001). Crystal structure of thermostable DNA photolyase: pyrimidine-dimer recognition mechanism. Proceedings of the National Academy of Sciences of the United States of America *98*, 13560-13565.

Kugler, J.E., Deng, T., and Bustin, M. (2012). The HMGN family of chromatin-binding proteins: dynamic modulators of epigenetic processes. Biochimica et Biophysica Acta *1819*, 652-656.

Lai, W., Li, H., Liu, S., and Tao, Y. (2013). Connecting chromatin modifying factors to DNA damage response. International Journal of Molecular Sciences *14*, 2355-2369.

Leibeling, D., Laspe, P., and Emmert, S. (2006). Nucleotide excision repair and cancer. Journal of Molecular Histology *37*, 225-238.

Lim, J.H., Bustin, M., Ogryzko, V.V., and Postnikov, Y.V. (2002). Metastable macromolecular complexes containing high mobility group nucleosome-binding chromosomal proteins in HeLa nuclei. The Journal of Biological Chemistry *277*, 20774-20782.

Lim, J.H., Catez, F., Birger, Y., West, K.L., Prymakowska-Bosak, M., Postnikov, Y.V., and Bustin, M. (2004). Chromosomal protein HMGN1 modulates histone H3 phosphorylation. Molecular Cell *15*, 573-584.

Lim, J.H., West, K.L., Rubinstein, Y., Bergel, M., Postnikov, Y.V., and Bustin, M. (2005). Chromosomal protein HMGN1 enhances the acetylation of lysine 14 in histone H3. The EMBO Journal *24*, 3038-3048.

Luger, K., Mader, A.W., Richmond, R.K., Sargent, D.F., and Richmond, T.J. (1997). Crystal structure of the nucleosome core particle at 2.8 A resolution. Nature *389*, 251-260.

Marteijn, J.A., Lans, H., Vermeulen, W., and Hoeijmakers, J.H. (2014). Understanding nucleotide excision repair and its roles in cancer and ageing. Nature Reviews Molecular Cell Biology *15*, 465-481.

Miller, K.M., Tjeertes, J.V., Coates, J., Legube, G., Polo, S.E., Britton, S., and Jackson, S.P. (2010). Human HDAC1 and HDAC2 function in the DNA-damage response to promote DNA nonhomologous end-joining. Nature Structural & Molecular Biology *17*, 1144-1151.

Morrison, A.J., and Shen, X. (2005). DNA repair in the context of chromatin. Cell Cycle *4*, 568-571.

Narlikar, G.J., Fan, H.Y., and Kingston, R.E. (2002). Cooperation between complexes that regulate chromatin structure and transcription. Cell *108*, 475-487.
Niida, H., and Nakanishi, M. (2006). DNA damage checkpoints in mammals. Mutagenesis *21*, 3-9.

Pao, G.M., Janknecht, R., Ruffner, H., Hunter, T., and Verma, I.M. (2000). CBP/p300 interact with and function as transcriptional coactivators of BRCA1. Proceedings of the National Academy of Sciences of the United States of America *97*, 1020-1025.

Peterson, C.L., and Cote, J. (2004). Cellular machineries for chromosomal DNA repair. Genes & Development *18*, 602-616.

Petruseva, I.O., Evdokimov, A.N., and Lavrik, O.I. (2014). Molecular mechanism of global genome nucleotide excision repair. Acta Naturae *6*, 23-34.

Pfeifer, G.P. (1997). Formation and processing of UV photoproducts: effects of DNA sequence and chromatin environment. Photochemistry and Photobiology *65*, 270-283.

Pilch, D.R., Sedelnikova, O.A., Redon, C., Celeste, A., Nussenzweig, A., and Bonner, W.M. (2003). Characteristics of gamma-H2AX foci at DNA double-strand breaks sites. Biochemistry and Cell Biology = Biochimie et Biologie Cellulaire *81*, 123-129.

Pogna, E.A., Clayton, A.L., and Mahadevan, L.C. (2010). Signalling to chromatin through post-translational modifications of HMGN. Biochimica et Biophysica Acta *1799*, 93-100.

Postnikov, Y.V., Belova, G.I., Lim, J.H., and Bustin, M. (2006). Chromosomal protein HMGN1 modulates the phosphorylation of serine 1 in histone H2A. Biochemistry *45*, 15092-15099.

Ramanathan, B., and Smerdon, M.J. (1989). Enhanced DNA repair synthesis in hyperacetylated nucleosomes. The Journal of Biological Chemistry *264*, 11026-11034.

Reeves, R. (2015). High mobility group (HMG) proteins: Modulators of chromatin structure and DNA repair in mammalian cells. DNA Repair.

Reeves, R., and Adair, J.E. (2005). Role of high mobility group (HMG) chromatin proteins in DNA repair. DNA Repair *4*, 926-938.

Richa, Sinha, R.P., and Hader, D.P. (2015). Physiological aspects of UV-excitation of DNA. Topics in Current Chemistry *356*, 203-248.

Riggs, P. (2001). Expression and purification of maltose-binding protein fusions. Current Protocols in Molecular Biology / edited by Frederick M Ausubel [et al] *Chapter 16*, Unit16 16.

Robert, C., and Rassool, F.V. (2012). HDAC inhibitors: roles of DNA damage and repair. Advances in Cancer Research *116*, 87-129.

Rogakou, E.P., Pilch, D.R., Orr, A.H., Ivanova, V.S., and Bonner, W.M. (1998). DNA double-stranded breaks induce histone H2AX phosphorylation on serine 139. The Journal of Biological Chemistry *273*, 5858-5868.

Sambrook, J., and Russell, D.W. (2006). Purification of nucleic acids by extraction with phenol:chloroform. CSH Protocols *2006*.

Sancar, G.B., and Smith, F.W. (1989). Interactions between yeast photolyase and nucleotide excision repair proteins in Saccharomyces cerevisiae and Escherichia coli. Molecular and Cellular Biology *9*, 4767-4776.

Sawan, C., and Herceg, Z. (2010). Histone modifications and cancer. Advances in Genetics *70*, 57-85.

Smerdon, M.J., Lan, S.Y., Calza, R.E., and Reeves, R. (1982). Sodium butyrate stimulates DNA repair in UV-irradiated normal and xeroderma pigmentosum human fibroblasts. The Journal of Biological Chemistry *257*, 13441-13447.

Smerdon, M.J., and Lieberman, M.W. (1978). Nucleosome rearrangement in human chromatin during UV-induced DNA- repair synthesis. Proceedings of the National Academy of Sciences of the United States of America *75*, 4238-4241.

Soria, G., Polo, S.E., and Almouzni, G. (2012). Prime, repair, restore: the active role of chromatin in the DNA damage response. Molecular Cell *46*, 722-734.

Spivak, G. (2015). Nucleotide excision repair in humans. DNA repair.

Subramanian, M. (2009). The role and molecular mechanism of HMGN proteins in global genome repair after UV irradiation. In Biology (Denton, Texas: Texas Woman's University), pp. 117.

Subramanian, M., Gonzalez, R.W., Patil, H., Ueda, T., Lim, J.H., Kraemer, K.H., Bustin, M., and Bergel, M. (2009). The nucleosome-binding protein HMGN2 modulates global genome repair. FEBS J *276*, 6646-6657.

Szyf, M. (2005). DNA methylation and demethylation as targets for anticancer therapy. Biochemistry Biokhimiia *70*, 533-549.

Tillhon, M., Cazzalini, O., Nardo, T., Necchi, D., Sommatis, S., Stivala, L.A., Scovassi, A.I., and Prosperi, E. (2012). p300/CBP acetyl transferases interact with and acetylate the nucleotide excision repair factor XPG. DNA Repair *11*, 844-852.

Tornaletti, S., and Hanawalt, P.C. (1999). Effect of DNA lesions on transcription elongation. Biochimie *81*, 139-146.

Trievel, R.C. (2004). Structure and function of histone methyltransferases. Critical Reviews in Eukaryotic Gene Expression *14*, 147-169.

Ueda, T., Postnikov, Y.V., and Bustin, M. (2006). Distinct domains in high mobility group N variants modulate specific chromatin modifications. The Journal of Biological Chemistry *281*, 10182-10187.

Ura, K., Araki, M., Saeki, H., Masutani, C., Ito, T., Iwai, S., Mizukoshi, T., Kaneda, Y., and Hanaoka, F. (2001). ATP-dependent chromatin remodeling facilitates nucleotide excision repair of UV-induced DNA lesions in synthetic dinucleosomes. The EMBO Journal *20*, 2004-2014.

Ura, K., and Hayes, J.J. (2002). Nucleotide excision repair and chromatin remodeling. European Journal of Biochemistry / FEBS *269*, 2288-2293.

van Attikum, H., and Gasser, S.M. (2005). The histone code at DNA breaks: a guide to repair? Nature Reviews Molecular Cell Biology *6*, 757-765.

van Hoffen, A., Venema, J., Meschini, R., van Zeeland, A.A., and Mullenders, L.H. (1995). Transcription-coupled repair removes both cyclobutane pyrimidine dimers and 6-4 photoproducts with equal efficiency and in a sequential way from transcribed DNA in xeroderma pigmentosum group C fibroblasts. The EMBO Journal *14*, 360-367.

van Steeg, H., and Kraemer, K.H. (1999). Xeroderma pigmentosum and the role of UV-induced DNA damage in skin cancer. Molecular Medicine Today *5*, 86-94.

Vempati, R.K., Jayani, R.S., Notani, D., Sengupta, A., Galande, S., and Haldar, D. (2010). p300-mediated acetylation of histone H3 lysine 56 functions in DNA damage response in mammals. The Journal of Biological Chemistry *285*, 28553-28564.

Volker, M., Mone, M.J., Karmakar, P., van Hoffen, A., Schul, W., Vermeulen, W., Hoeijmakers, J.H., van Driel, R., van Zeeland, A.A., and Mullenders, L.H. (2001). Sequential assembly of the nucleotide excision repair factors in vivo. Molecular Cell *8*, 213-224.

Wang, H., Zhai, L., Xu, J., Joo, H.Y., Jackson, S., Erdjument-Bromage, H., Tempst, P., Xiong, Y., and Zhang, Y. (2006). Histone H3 and H4 ubiquitylation by the CUL4-DDB-ROC1 ubiquitin ligase facilitates cellular response to DNA damage. Molecular Cell *22*, 383-394.

Watson J.D., B.T.A., Bell Stephen P., Gann Alexander, Levine Michael, and Losick Richard (2014). Molecular Biology of the Gene, J. SMith, ed.

Wyrick, J.J., and Roberts, S.A. (2015). Genomic approaches to DNA repair and mutagenesis. DNA Repair.

Xie, Z., Liu, S., Zhang, Y., and Wang, Z. (2004). Roles of Rad23 protein in yeast nucleotide excision repair. Nucleic Acids Research *32*, 5981-5990.

Yarosh, D.B. (2004). DNA repair, immunosuppression, and skin cancer. Cutis *74*, 10-13.

Yodh, J. (2013). ATP-Dependent Chromatin Remodeling. Advances in Experimental Medicine and Biology *767*, 263-295.

Yu, S., Teng, Y., Waters, R., and Reed, S.H. (2011). How chromatin is remodelled during DNA repair of UV-induced DNA damage in Saccharomyces cerevisiae. PLoS Genetics *7*, e1002124.

Yu, Y., Deng, Y., Reed, S.H., Millar, C.B., and Waters, R. (2013). Histone variant Htz1 promotes histone H3 acetylation to enhance nucleotide excision repair in Htz1 nucleosomes. Nucleic Acids Research *41*, 9006-9019.

Yu, Y., Song, C., Zhang, Q., DiMaggio, P.A., Garcia, B.A., York, A., Carey, M.F., and Grunstein, M. (2012). Histone H3 lysine 56 methylation regulates DNA replication through its interaction with PCNA. Molecular Cell *46*, 7-17.

Yu, Y., Teng, Y., Liu, H., Reed, S.H., and Waters, R. (2005). UV irradiation stimulates histone acetylation and chromatin remodeling at a repressed yeast locus. Proceedings of the National Academy of Sciences of the United States of America *102*, 8650-8655.

Zhang, Q., and Wang, Y. (2008). High mobility group proteins and their post-translational modifications. Biochimica et Biophysica Acta *1784*, 1159-1166.

Zotter, A., Luijsterburg, M.S., Warmerdam, D.O., Ibrahim, S., Nigg, A., van Cappellen, W.A., Hoeijmakers, J.H., van Driel, R., Vermeulen, W., and Houtsmuller, A.B. (2006). Recruitment of the nucleotide excision repair endonuclease XPG to sites of UV-induced dna damage depends on functional TFIIH. Molecular and Cellular Biology *26*, 8868-8879.

APPENDIX

LIST OF ABBREVIATIONS

LIST OF ABBREVIATIONS

6-4PPs – pyrimidine (6-4) pyrimidone photo products

Ac – Acetyl

ACF – ATP-dependent chromatin remodeling factor

Ac-H3K9 – acetylated histone H3 lysine 9

Amp – Ampicillin

ANOVA – Analysis of variance

ATP – Adenosine triphosphate

BRCA1 – Breast cancer 1, early onset

CETN2 – centrin, EF-hand protein, 2

CMV – Cytomegalovirus

Co-IP – Co-immunoprecipitation

CP – Xeroderma pigmentosum

CPDs – Cyclobutane pyrimidine dimers

CS – Cockyane Syndrome

CUL4-DDB-ROC1 – Ubiquitin ligase

DDB1/2 – Damaged DNA binding complex

DNA - Deoxyribonucleic acid

DSB – Double strand break repair

ERCC1 – Excision repair cross complementing protein 1

FITC – Fluorescein isothiocyanate

GCN5 – General control of amino acid synthesis 5 (histone acetyl transferase)

GFP – Green fluorescent protein

GGR – Global genome repair

H1 – Linker histone

H2/H3/H4 – Core histones

H2A.Z – Histone 2 variant

H3K14 – Histone H3 lysine 14

H3K9 – Histone H3 lysine 9

H4K5 – Histone H4 lysine 5

HA tag – Human influenza hemagglutinin tag

HAT – Histone acetyltransferase

HDAC – Histone deacetylase

HeLa-tag – HeLa cells expressing basal levels of HMGN1 and HMGN2

HeLa HMGN1-tag – human HeLa cells overexpressing HMGN1 protein

HeLa HMNG2-tag – human HeLa cells overexpressing HMGN2 protein

hHr23B – Human homologue of the yeast protein RAD23B

HMGA – High mobility group AT-hook protein

HMGB – High mobility group box protein

HMGN – High mobility group nucleosomal protein

Hybond N^+ - Positively charged nylon membrane

IgG – Immunoglobin

IL-2 – Interleukin 2

IMR-90 - Human foetal lung fibroblast cells

IP – Immunoprecipitation

IPTG - Isopropyl β-D-1-thiogalactopyranoside

ISWI – Imitation SWItch (yeast)

LB – Lysogeny broth

LD_{50} – Lethal dose, 50%

LSD1 – Lysine (K)-specific demethylase 1A

MBP – Maltose binding protein

MEF – Mouse embryonic fibroblast

MFA2 – Mating pheromone A factor

Mi-2 – part of NURD complex, ATP-dependent chromatin remodeler

NEIL 2 – Nei like-2 protein, a DNA glycosylase/AP lyase specific

NER – Nucleotide Excision Repair

N-terminal – Amino terminal

P300 – E1A binding protein p300

P53 – Tumor suppressor protein

PAGE – Polyacrylamide gel electrophoresis

PBS – Phosphate buffer saline

PCNA – Proliferating cell nuclear antigen

PCR – Polymerase chain reaction

RBX1 – RING-box protein 1

Rec – Recombinant

RIPA – Radio immunoprecipitation assay

RNA-Pol II – Ribonucleic acid polymerase II

SD – Standard deviation

SDS-PAGE – Sodium dodecyl sulfate polyacrylamide gel electrophoresis

SE – Standard error

Sin3p/Rpd3p – Histone deacetylase complex in yeast

SNF – Sucrose nonfermenting (yeast)

SWI – Switching (yeast)

Swi2p – ATP-dependent chromatin remodeling complex

TCR – Transcription couple repair

TTD - Trichothiodystrophy

UV – Ultra violet

UVC – Ultraviolet subtype C

WB – Western blot

X-Gal - 5-bromo-4-chloro-3-indolyl-β-D-galactopyranoside

XP – Xeroderma pigmentosum

XPA, B, C, D, E, F, G, H - Xeroderma pigmentosum protein